FINAL REPORT: 27 FEBRUARY 2003

RESUTLS FROM THE INDICES WORKING GROUP ON THE DEVELOPMENT AND USE OF ENVIRONMENTAL INDICES IN THE PREDICTION OF POLLOCK RECRUITMENT IN THE EASTERN BERNING SEA

Edited By J. D. Schumacher

With contributions from

Nick Bond, Al Hermann, Anne Hollowed, Jim Ianelli, Nancy Kachel, Carol Ladd, Pat Livingston, Allen Macklin, Bern Megrey, Jeff Napp, Dylan Ridgi, Sigrid Salo, Jim Schumacher, Alan Springer, Phyllis Stabeno, and Peggy Sullivan.

TABLE OF CONTENTS

1. **INTRODUCTION**

The goal of the Southeast Bering Sea Carrying Capacity (SEBSCC) program is to document the role of juvenile pollock in the eastern Bering Sea ecosystem. This includes examination of factors that affect their survival and development and testing of annual indices of pre-recruit (age -1) abundance (from the SEBSCC Concept Paper, July 1995). Within this framework, the purpose of the Indices Working Group (IWG, which was developed at the SEBSCC Principal Investigators meeting held in January 2001) is as follows. Based on the best understanding of ecosystem dynamics, identify potential single- or multi-parameter constructs or indices (e.g., wind mixing, time of spring bloom, etc.) that lead to development of survival indices for pollock in the egg, larval and young of the year life history stages. This information will provide input to the National Marine Fisheries Service (NMFS) stock assessment model and/or models of juvenile pollock for use by fisheries scientists at the Alaska Fisheries Science Center (AFSC)/NMFS.

2. **CONCEPTUAL FRAMEWORK FOR DEVELOPMENT OF INDICES**

2.1 A Pollock-centric Perspective of the Southeastern Bering Sea Ecosystem.

As noted by Napp et al (2000) pollock is the most abundant species harvested in the Bering Sea, accounting for > 65% of the total groundfish biomass and during the 1980s when their total biomass exceeded 20 million tones. The biomass trends of three major trophic guilds in the eastern Bering Sea (1979 to 1998: Schumacher et al., in press) show that while the total biomass of pollock in the 1990s is less than in the 1980s, they still dominate biomass in any of the guilds which include marine birds, mammals, other fishes and crabs. Walleye pollock is a nodal species in the food web (NRC Report, 1996) with juveniles being the dominant prey of fishes, seabirds, and marine mammals (Springer and Byrd, 1989; Livingston, 1993; Brodeur *et al.*, 1996). It is natural that that pollock have been the focus of the Coastal Ocean Program's SEBSECC. The choice of developing a survival index for the early life history stages (eggs through young of the year) allows an early forecast of potential recruitment to the fishery and a metric that can be compared to existing time series of age-1 abundance (Figure 1).

RECRUITMENT BY YEARCLASS
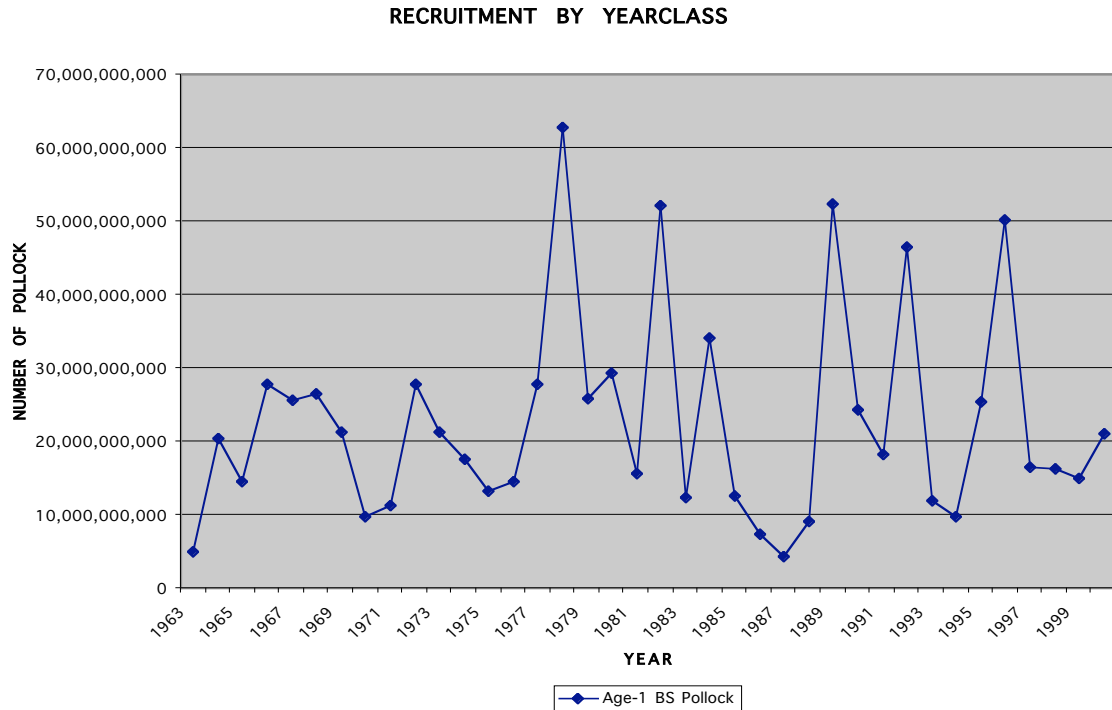
Figure 1. Recruitment of age-1 pollock in the eastern Bering Sea estimated as number of fish (from SAFE Report 2001).

A switch model was developed for the eastern Bering Sea (Megrey et al., 1996), which identifies candidates for causing mortality by life history stage and the mortality variability of each stage indicating the stage contributing the most variability in recruitment to the fishery is set (Figure 2).   In this model, transport and turbulence have their greatest impact on mortality of yoke-sack through feeding larval stages. It is the vertical structure of temperature, however, through its suggested influence on cannibalism that has the greatest impact on recruitment (see **Section 4** for more detail on egg/larval transport and the subsequent potential impact on cannibalism).

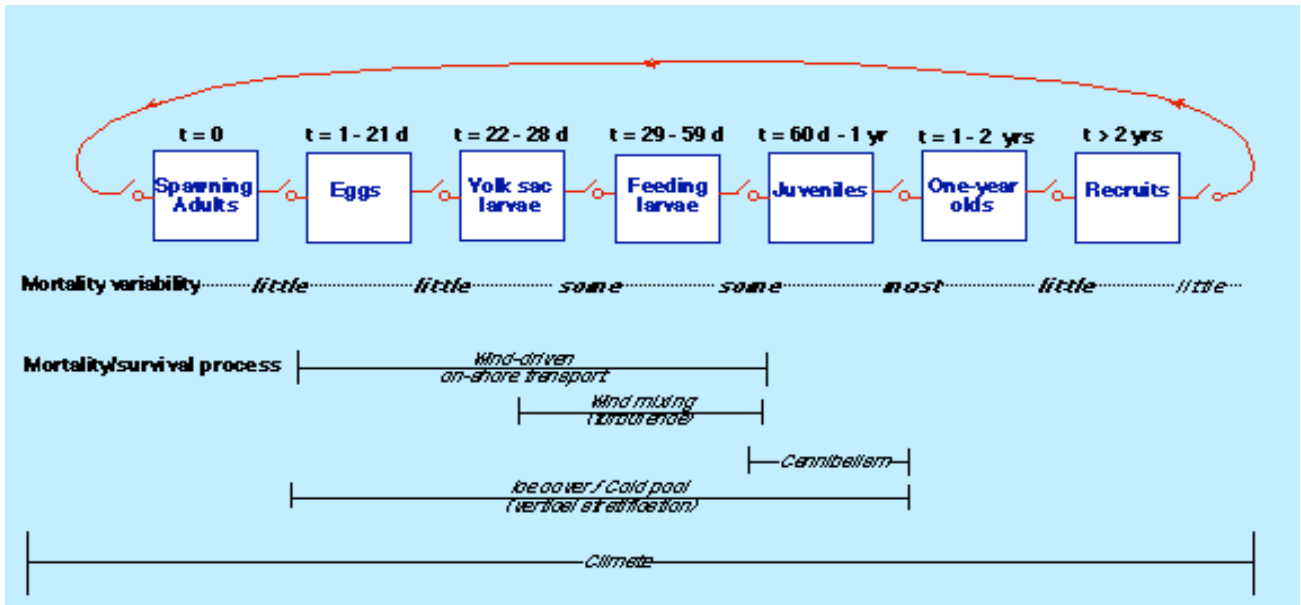Figure 2. Switch model of pollock dynamics in the eastern Bering Sea. Processes though to be important regulators of survival variability are shown and the span of their interaction is indicated.

In a later version of the switch model, Napp et al. (2000) augmented the candidates that regulate survival by adding the timing of preferred prey production and the absence or presence of ice over the shelf region. Most recently, these have been woven together with other environmental factors to develop the Oscillating Control Hypothesis (OCH), which examines how energy flow through the ecosystem varies in different climate regime (Hunt et al., in press).

2.2 A Generic Model of Pathways of Energy Flow through the Ecosystem

Although the focus on pollock is reasonable and models that have pollock as the central feature helped focus research in SEBSCC, a more inclusive perspective also has value. This is particularly true when considering question on the ecosystem scale, e.g., the dramatic decline in abundance of the Steller sea lion. Identifying and understanding mechanisms that transfer climate change via the ocean to biota is essential if we are to understand ecosystem dynamics (Francis *et al.*, 1998). Fluctuations in the physical environment can impact the ecosystem through both changes in the nutrient-phytoplankton-zooplankton sequence (i.e.,

bottom-up control), and/or by altering habitat resulting in changes in abundance and/or composition of higher trophic level animals (i.e., top-down control). Hunt et al. (in press) hypothesize that the control of energy flow on the shelf (either top down or bottom up) depends on the timing of the nutrient-phytoplankton-zooplankton sequence related to the presence/absence of sea ice.

More inclusive and general conceptual models have been developed for the eastern Bering Sea and North Pacific Ocean. Schumacher et al. (in press) adapted the Francis et al. (1998) conceptual model of the pathways that climate phenomenon influence the biota to include sea ice, a dominant feature of the ecosystem of the eastern Bering Sea shelf (Figure 3).
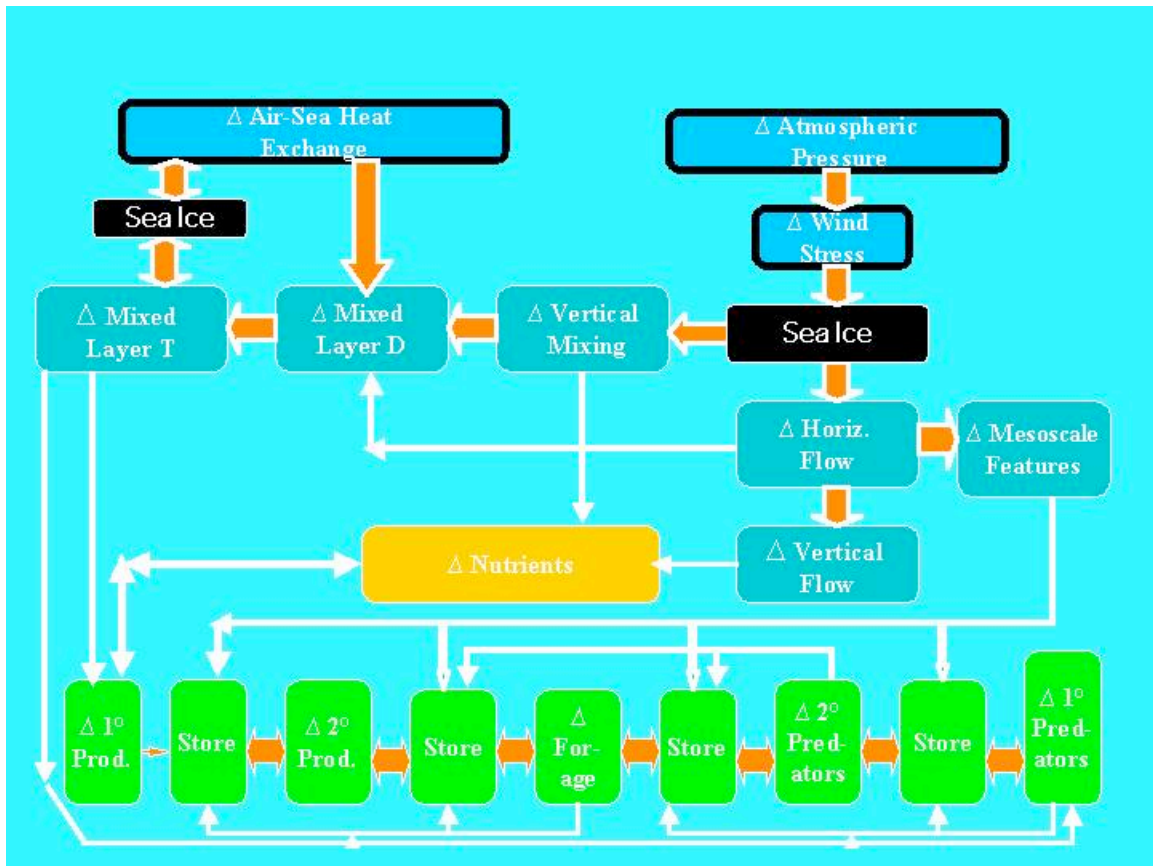
Figure 3. Conceptual model showing the pathways through which changes in atmospheric features can influence oceanic and biological components of the ecosystem of the eastern Bering Sea (from Schumacher et al., in press)

This model shows that there are numerous ecosystem elements (Section 5 discusses relationships between adjacent and more widely separated ecosystem elements) and connecting processes to consider when attempting to understand the impact of changes in atmospheric pressure on survival of young pollock. For example, a change in characteristics of the Aleutian Low will alter wind stress and the ensuing horizontal flow field (upper layer currents), it also will impact vertical mixing and air-sea heat fluxes and thereby the temperature of the upper mixed layer.   These changes in transport, turbulence and temperature can impact the biological ecosystem element of interest either by enhancing or limiting survival, or both.

2.3 Other Aspects of Indices Development

As expected, many questions were generated and addressed during IWG workshops. One area of critical interest related to the potential time/space scale mismatch or match among features of the ecosystem. From a physics perspective, the eastern shelf has distinct regions or strata that are dominated by different physical processes. This is strongly evident in an across-shelf direction going from the more oceanic-like outer shelf waters to the strongly two-layered middle shelf and then shoreward into a water column that often is without vertical structure. More recent results (Stabeno et al., in press) show difference in advection occurs within the previously defined latitudinal strata (southeastern, central and northern shelf, Schumacher and Stabeno, 1998). For this reason, some of the physical observations were partitioned into areas within the NMFS strata (Section 3.4). Some data sets, however, would become too noisy if the spatial domain is reduced some limit. For example, the estimates of pollock abundance from the bottom trawl survey can be grouped in the same areas (Figure 4) used for the ice index. It was the consensus of the IWG that this time series contains too much variation and that
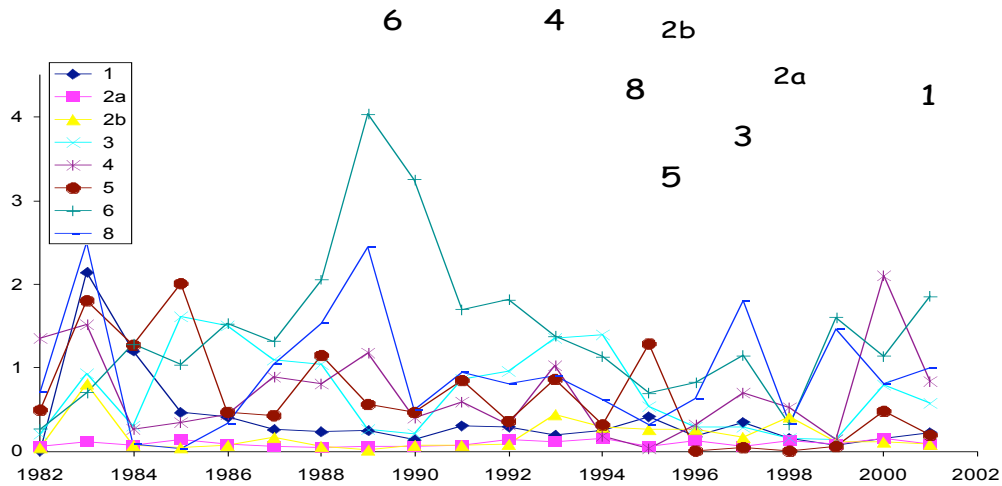
Figure 4. Abundance of adult pollock in the unequal areas used in the development of the ice index (Section 3.4)

the integrated values (i.e., the commonly used time series of adult or age-1pollock throughout the eastern Bering Sea) provided the appropriate time series of abundance.

The IWG members also felt that it was important to consider the local/regional impact of larger scale indices went seeking relationships between physics and biology. For example, when using a hemispherical index (e.g., Arctic Oscillation, PDO, NPI), one should first consider how it is manifest on the regional or local scale. This also applies on finer spatial scales, e.g., how representative are measured winds at St. Paul Island to mixing processes in inner Bristol Bay? While zeroth order approaches have some value, their results can be misleading. For example, several studies use the OSCURS model to transport planktonic stages of various species. In this simulations, only on relase site is used to initialize trajectories. As results from the NEPROMS have shown (Section 3.7), changes in initial location can result in significantly different trajectories.

3. 1 DEVELOPMENT OF ENVIRONMENTAL INDICES

[To be completed by appropriate IWG members]

3.1 Indices of stratification, potential supply of nutrients to the upper mixed layer and turbulence experienced by larval pollock by Carol Ladd and Phyllis Stabeno.

We used the Price-Weller-Pinkel (Price *et al*., 1986) one-dimensional mixed layer model to simulate the establishment of stratification and subsequent mixing over the southeast Bering Sea shelf during summer. We selected the location, 56.9ºN, and 164.1ºW, to coincide with the site of FOCI biophysical Mooring 2. Observations collected at this mooring provide 7 years of data that were used to validate model results.

The model calculates the density and wind-driven velocity profile in response to imposed atmospheric forcing (discussed below). Vertical mixing occurs in order to satisfy three stability criteria:

1. static stability: $\dfrac{\partial \rho}{\partial z} \geq 0$,

2. mixed layer stability: $R_b \equiv \dfrac{g \Delta \rho\, h}{\rho_0 (\Delta V)^2} \geq 0.65$,

3. shear flow stability: $R_g \equiv \dfrac{g\, \partial \rho / \partial z}{\rho_0 \left(\partial V / \partial z \right)^2} \geq 0.25$,

where h is the mixed layer depth and $\Delta \rho$ (ΔV) is the difference in density (velocity) between the mixed layer and the level just beneath (Price *et al*., 1986). Whenever, any of these criteria are violated, the model mixes properties at neighboring (in the vertical) points on the model grid until the criteria are satisfied. The model was run with a vertical resolution of $\Delta z = 1.0$ m to a depth of 72 m and a time step of $\Delta t = 864$ seconds. Model simulations were initialized with a vertical temperature profile derived from the NCEP Reanalysis (Kalnay *et al*., 1996). We used the sea surface temperature (SST) from May 1 combined with a weak thermocline ($\Delta T = 0.5$ºC) between 10 and 20 m. The model is then forced with winds and heat fluxes from the reanalysis, and run from May 1 through September 30 of each year.

Comparisons with data show that the model reproduces mixed layer depth, and timing of stratification set-up and mixing events quite well.

The following assumptions and caveats should be noted:

The model is one-dimensional. Hence, advection is assumed to be unimportant. Advection over the middle shelf is generally weak (Schumacher and Kinder, 1983, Schumacher and Stabeno, 1998). At times, however, currents have resulted in transport of salt and nutrients at this location (Stabeno et al, 2001). In general, the assumption of no advection is likely good at this site, but it would have to be evaluated for other locations.

The model is initialized with May 1 SST from the NCEP reanalysis. This time series has errors on the order of ±0.5°C when compared to in situ observations collected at site 2 between 1996-2001. These errors are well within the magnitude of interannual variability in the NCEP SST (the standard deviation over 40 years is ~ 1°C). Summer heat content and SST of the model results, however, are dependent on the initial temperature profile and will reflect errors in that profile.

Based on comparisons between model simulations and observations at site 2, salinity appears to have only a minor impact on stratification and mixing processes. Waters of the middle shelf domain exhibit weak horizontal and vertical gradients in salinity (Coachman, 1986), and the time series of salinity measurements are sparse. Therefore salinity is kept constant (31.65 psu) throughout the model runs.

The model includes a diffusive term that results in a slightly weaker thermocline than observed. Without diffusion, the thermocline becomes too strong resulting in SSTs that are too warm.

Although the model simulates mixing processes in the upper layer quite well, the bottom mixed layer is not reproduced. Over the middle shelf, the water column exhibits a strongly stratified two-layer structure (in temperature) with a wind-mixed surface layer and a tidally mixed bottom layer (Schumacher and Stabeno, 1998). The model does not include any tidal mixing.

Results

Interannual variability in mixing conditions can be evaluated using the model hindcasts. Model results show that the stratification maximum during May/June of each summer has varied on an approximately decadal time scale (Fig. 1) with maxima in 1967, the early 1980's, and 1997 and minima in the early 1970s and late 1980s. We note that this signal is not in phase with the accepted regime shifts (1976/77, 1989 and perhaps 1998) observed in physical and biological time series for the eastern Bering Sea (Hare and Mantua, 2001).
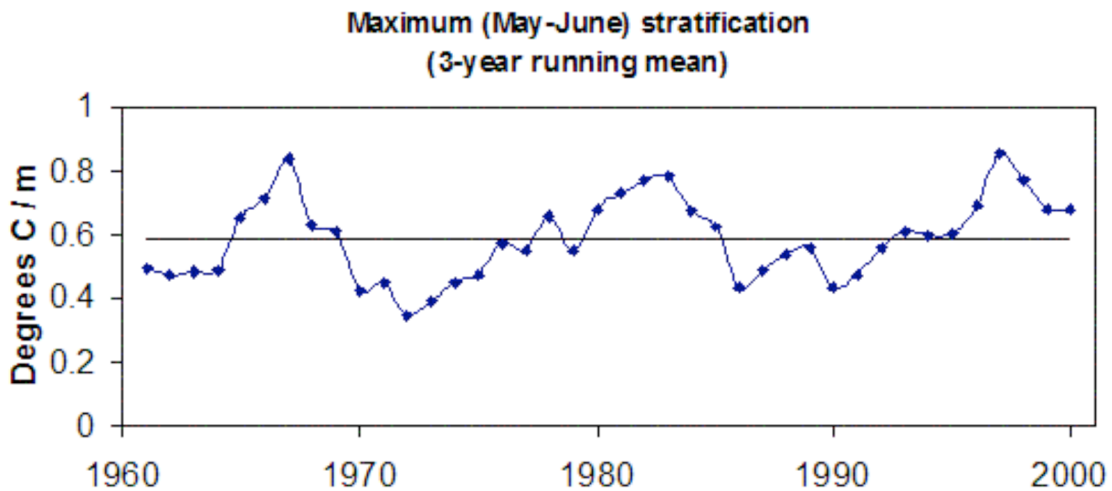
Figure 1. Maximum over May/June of vertical stratification maximum.

When stratification is established in the spring provides an index of the timing of the spring bloom (Fig. 2) based on classical critical depth theory (Sverdrup, 1953). Interannual variability in the date of stratification is high with little indication of variability on decadal time scales. The stratification date averages 18 May and ranges between 10 May and 25 June.
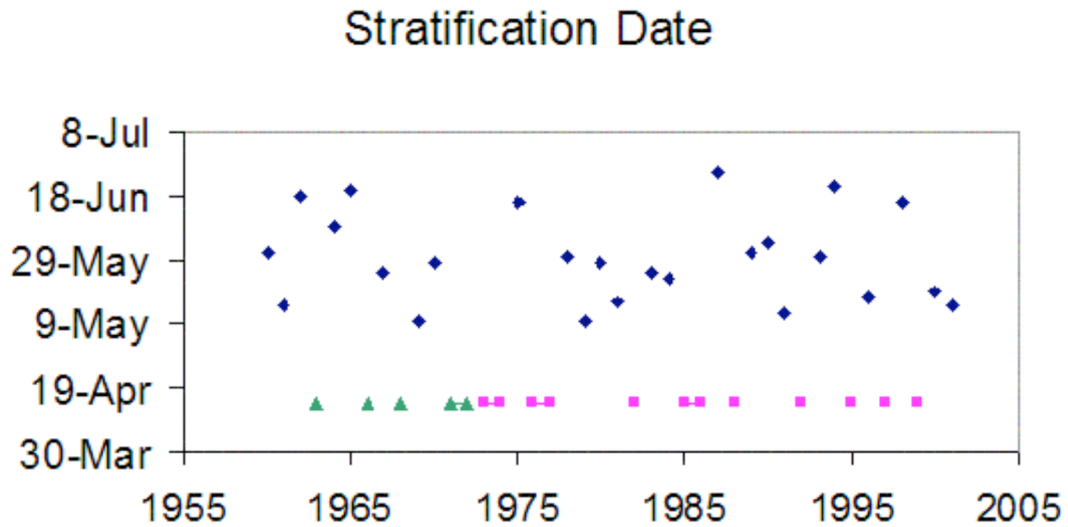
Figure 2. Date when Max Dtemp/Dz first > 0.2 ºC/m and Depth of Max < 25m, for more than 1 day. Pink squares (ice data based on satellite images) and green triangles (ice data based on shipboard observations) represent years when there was ice after April 1 and an ice-associated bloom would be expected (Stabeno et al, 2001).

The number of mixing events over the summer (Fig. 3) provides both an index of the potential (some nutrients must still exist in the lower layer) amount of nutrient entrained into the mixed layer and of conditions that relate to decreased survival of pollock larvae (Bailey and Macklin, 1994). A high number of mixing events in a given year may indicate higher primary production and increased mortality of pollock larvae.
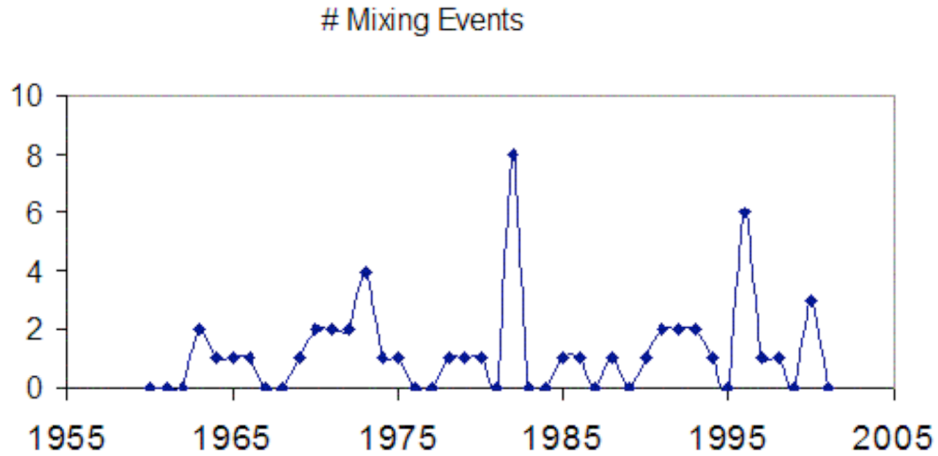
Figure 3. Number of times between the stratification setup date and 31 Aug when 3-day smoothed MLD increases > 5 m in a day.

Temperature is important to the development of pollock eggs with eggs being slower to hatch in colder conditions (Blood, 2002). Temperature also affects the production of zooplankton (Hunt et al, in press). The water column temperature on the stratification date (Fig. 4) may influence the coupling between the spring phytoplankton bloom and zooplankton prey for first feeding and older larvae. Water column temperature on the stratification date varies between less than 1°C in 1991 to over 4°C in 1987 with high interannual variability, especially after 1980.
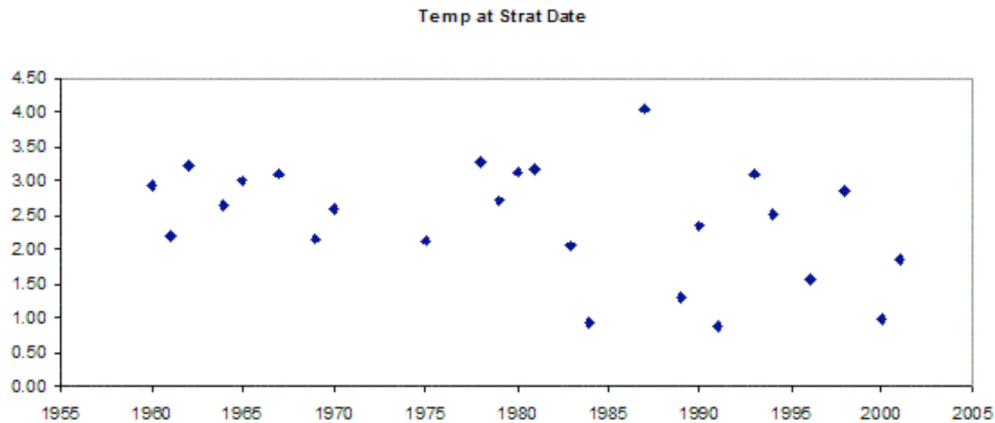
Figure 4. Water column average temperature on the stratification date. No temperature is shown for years when ice was present after April 1.

Future work

In order to expand on the present results, the model is being modified to track entrainment of water into the mixed layer. This will enable quantitative estimates of nutrient flux into the mixed layer over the summer. Another option would be to include a nutrient-like tracer, kept constant in the bottom layer and depleted over some time scale in the mixed layer.

References

Bailey, K.M. and S.A. Macklin, 1994. Analysis of patterns is larval walleye pollock *Theragra chalcogramma* and wind mixing events in Shelikof Strait, Alaska. *Mar. Ecol. Pro. Ser. 113*, 1-12.

Blood, D. M., 2002: Low-temperature incubation of walleye pollock (Theragra chalcogramma) eggs from the Southeast Bering Sea shelf and Shelikof Strait, Gulf of Alaska. *Deep-Sea Research II: Topical Studies in Oceanography*, submitted.

Coachman L.K., 1986. Circulation, water masses, and fluxes on the southeastern Bering Sea shelf. *Cont. Shelf. Res., 5,* 23-108.

Hare, S.R., and N.J. Mantua, 2001. Empirical evidence for North Pacific regime shifts in 1977 and 1989. *Prog. Oceanogr. 47,* 103–146.

Hunt, G.L., Jr., P. Stabeno, G. Walters, E. Sinclair, R.D. Brodeur, J.M. Napp, and N.A. Bond, in press. The Eastern Bering Sea: evidence for change and a new hypothesis linking ecosystem control and climate. *Deep-Sea Res. II.*

Kalnay, E., M. Kanamitsu, R. Kistler, W. Collins, D. Deaven, L. Gandin, M. Iredell, S. Saha, G. White, J. Woollen, Y. Zhu, A. Leetmaa, B. Reynolds, M. Chelliah, W. Ebisuzaki, W. Higgins, J. Janowiak, K. C. Mo, C. Ropelewski, J. Wang, R. Jenne, and D. Joseph, 1996: The NCEP/NCAR 40-Year Reanalysis Project. *Bull. Am. Met. Soc.*, **77,** 437–472.

Price, J. F., R. A. Weller, and R. Pinkel, 1986: Diurnal cycling: observations and models of the upper ocean response to diurnal heating, cooling and wind mixing. *J. Geophys. Res.*, **91,** 8411-8427.

Schumacher, J.D. and T.H. Kinder, 1983. Low frequency currents over the Bering Sea Shelf. *J. Phys. Oceanogr., 13,* 607-623.

Schumacher, J. D. and P. J. Stabeno, 1998: The continental shelf of the Bering Sea. *The Sea: The global coastal ocean: regional studies and synthesis*, A. R. Robinson and K. H. Brink, Eds., John Wiley and Sons, 789-822.

Stabeno, P.J., N. A. Bond, N. B. Kachel, S. A. Salo, and J. D. Schumacher, 2001. Temporal Variability in the Physical Environment over the Southeastern Bering Sea. *Fish. Oceanogr., 10*: 81-98.

Sverdrup, H.U., 1953. On conditions for the vernal blooming of phytoplankton. *J. Conseil Exp. Mer 18,* 287-295.

3.2 An Index Related To Wind Turbulence and Feeding Success by Bern Megrey and Nick Bond

Using a process oriented IBM of pollock fish larvae, which incorporated a detailed description of the turbulence/contact rate/feeding success process (Megrey and Hinckley 2001), we evaluated the relationship between the model predicted influence of wind-generated turbulence on feeding. Output from the model (Figure 1 and 2) conforms nicely to the theory by the indication of a well-defined peak in consumption at intermediate wind speeds (MacKenzie *et al.*, 1994). Because of the high variability in the model data, we estimated the wind speed that generated optimum consumption by fitting a quadratic line through wind speed and consumption data, averaged by Julian day over the period DOY 102-164, the period when larvae pollock are alive (Figure 3). The wind speed that generated maximum consumption was derived by taking the derivative of the fit quadratic equation and setting it to zero. Optimum feeding was (540 µg dry weight per day per individual) at a wind speed of 7.1 m·s⁻¹ indicated in Figure 1 by a solid red circle.
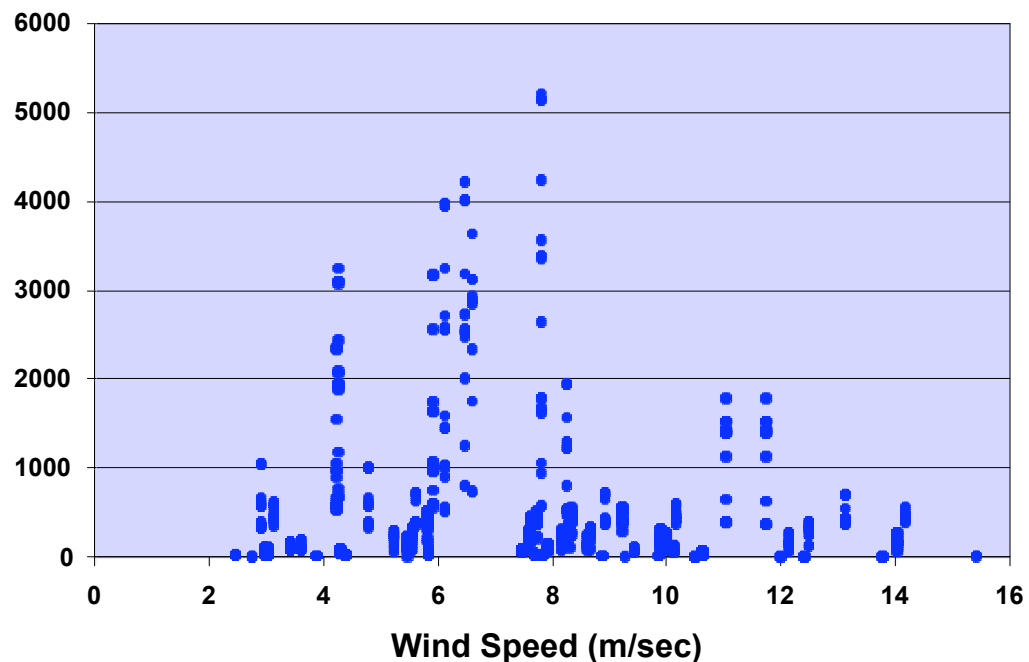

Figure 1. IBM output showing consumption as a function of wind speed
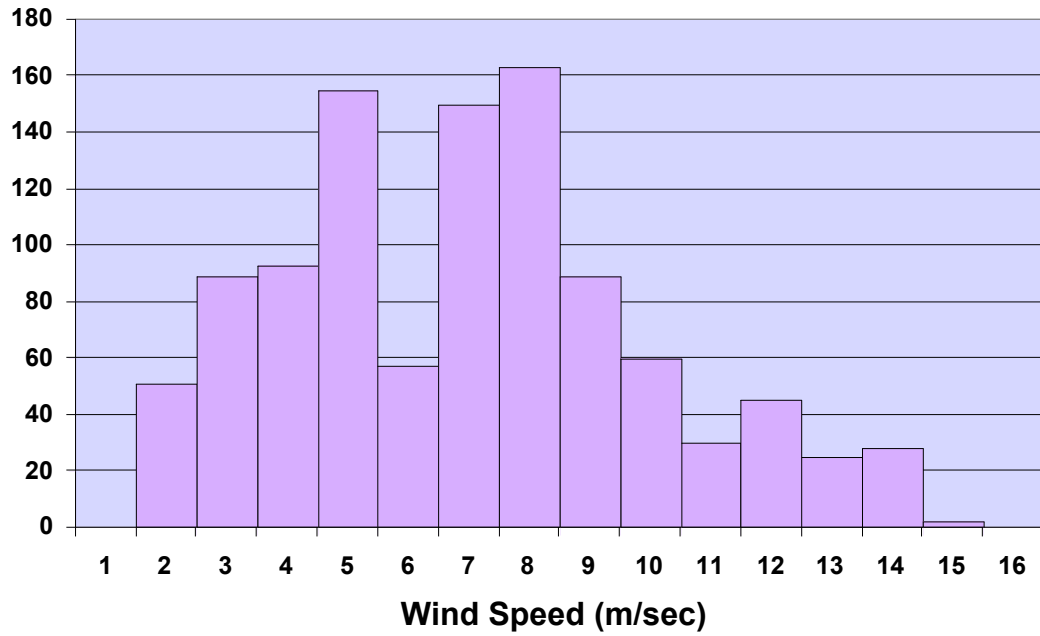
Figure 2. Frequency histogram of wind speeds used to force the IBM model.
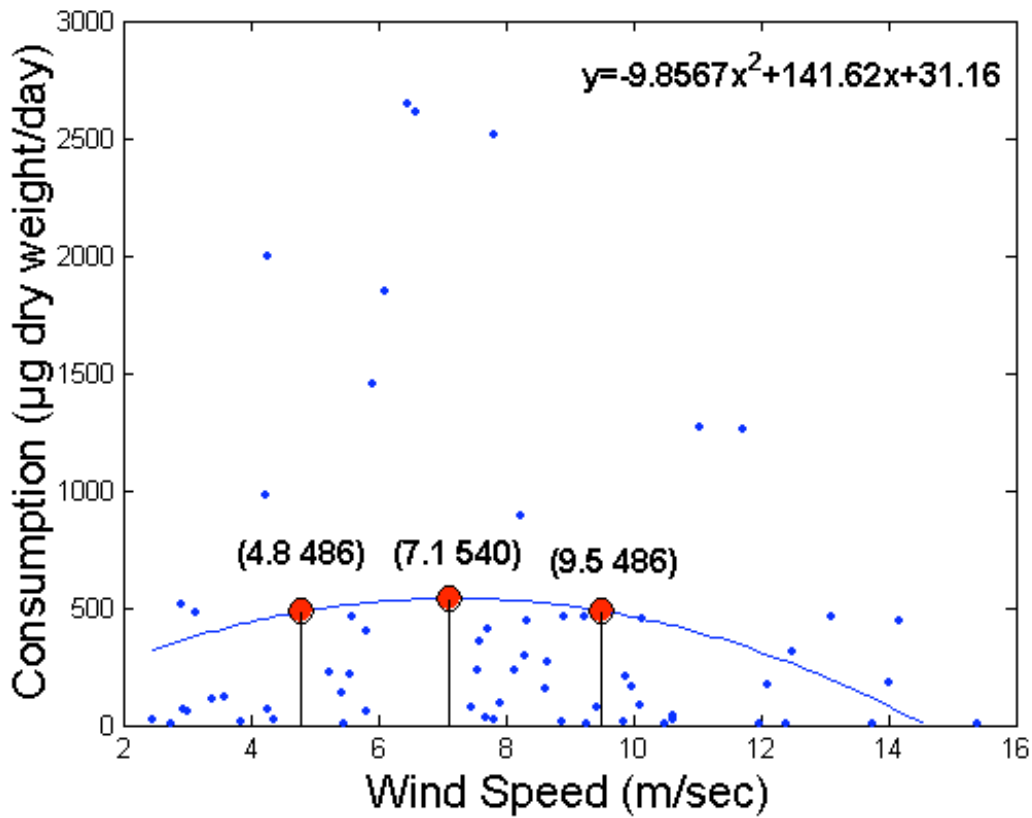
Figure 3. Estimates of the wind speeds required to generate optimum feeding

Using Figure 3, we arbitrarily defined the range of optimum feeding to be ± 15% of the optimum level. (486 μg dry weight per day per individual). The wind speeds corresponding to a feeding level of 486 were 4.8 and 9.5 m·s⁻¹. These points are indicated in Figure 3 with solid red circles. Thus the range of wind speeds that that provide "favorable feeding" would be 4.8 to 9.5 ms⁻¹. At wind speeds > 9.5 ms⁻¹ increased turbulence negatively affects feeding and at wind speeds < 4.8 ms⁻¹ feeding is less than optimal because wind speed are not sufficient to enhance contact rate.

Caveats: Results are from a model experiment not laboratory experiment. Simulations were carried out on Shelikof Strait walleye pollock. However results should be applicable to Bering Sea pollock as the feeding/contact rate/turbulence processes should still be valid. Wind induced turbulence was not the only major process in the IBM model. The IBM was

very detailed and included many other biological process which would have affected the outcome of the simulations.

Megrey, B.A. and S. Hinckley 2001. Effect of turbulence on feeding of larval fishes: a sensitivity analysis using an individual-based model. ICES Journal of Marine Science 58:1015-1029

MacKenzie, B. R., Miller, T. J., Cyr, S., and Leggett, W. C. 1994. Evidence for a dome-shaped relationship between turbulence and larval fish ingestion rates. Limnology and Oceanography, 39(8): 1790-1799.

3.6 Model Simulations Or What Is NEPROMS? by Al Hermann

The Regional Ocean Modeling System (ROMS) is a versatile, state-of-the-art, free-surface, hydrostatic primitive equation ocean circulation model developed at Rutgers University and UCLA, for both single and multi-threaded computer architectures. As its predecessors (SCRUM and SPEM), ROMS is terrain-following, and is discretized in space on an orthogonal curvilinear, Arakawa C-grid, and in time using optional third- order, split-explicit time stepping algorithms. System attributes include extensive restructuring for sustained performance on parallel-computing platforms; high-order, weakly dissipative algorithms for tracer advection; a unified treatment of surface and bottom boundary layers, based on the Large *et al*. (KPP) and Styles and Glenn (bottom boundary layer) algorithms; an integrated set of procedures for data assimilation (*e.g*., optimal interpolation, reduced-state Kalman filter, and adjoint-based methods); and advanced treatments of open boundary conditions. Numerical details can be found in Haidvogel et al. (2000), Shchepetkin and McWilliams (1998) and Marchesiello *et al*. (2001), and on the ROMS web site (http://marine.rutgers.edu/po/index.php). The ROMS user community now numbers more than 200 scientists world-wide.

The version of ROMS used for our simulations achieves distributed memory parallelism using the Scalable Modeling System developed at NOAA's Forecast Systems Laboratory. SMS is a set of high level tools designed to simplify the parallelization of structured grid

codes, as well as to address parallel coding issues including data decomposition, loop translations, data movement, reductions, and parallel debugging. The user inserts directives in the form of comments into existing FORTRAN code. SMS translates the code and directives into a parallel version that runs efficiently on both shared and distributed memory high-performance computing platforms. The parallel code is built on top of the Message Passing Interface Library (MPI), enabling it to be fully portable. On shared memory machines, comparable shared memory libraries may also be used to implement the message passing functionality. While the tool has been tailored toward finite difference and spectral atmospheric and ocean models, the approach is sufficiently general to be applied to other structured grid codes. SMS has been shown to compare favorably with hand-coded MPI timings on many geophysical applications.

Using this parallel version of ROMS, we have been implementing a suite of basin-, regional-, and local-scale circulation models, linked via one- (and eventually two-) way coupling. Figure 1 shows the set of nested modeling domains in current use, including: a basin-scale model encompassing the North Pacific Basin at 20-40 km resolution (NPac), a regional model at ~10 km resolution spanning the Northeast Pacific (NEP), and finally local models at ~3 km resolution in regions of specific interest [California Current System (CCS) and the Coastal Gulf of Alaska (CGOA)]. The NEP grid spans the area from Baja California up through the Bering Sea at approximately 10 km resolution, and was used for the simulations of the Bering Sea reported here. Additional information on these models (with snapshots and animations of model output) are available at http://www.pmel.noaa.gov/~dobbins/nep.html.

This figure is attached as Fig 1 nested NEPROMS (PDF FILE from Al Hermann)

Figure 1. Nested modeling domains in current use for Pacific modeling, including: a basin-scale model encompassing the North Pacific Basin at 20-40 km resolution (NPac, red), a regional model at ~10 km resolution spanning the Northeast Pacific (NEP, green), and finally local models at ~3 km resolution in regions of specific interest [California Current System (CCS, light blue) and the Coastal Gulf of Alaska (CGOA, light blue)].

The NEP model is forced with daily average wind (converted to wind stress) and heat fluxes (sensible, latent, longwave and shorwave) from the NCEP reanalysis project. No tidal forcing is included in these simulations. Model runs were initialized with Levitus monthly climatology for T and S fields. Hindcasts for a particular year were achieved by spinning up the NEP model from January of the previous year; for example, the model was spun up using daily NCEP values from January 1999 – March 2000 for hindcasts of the period April-July 2000. Although even longer spinup would be preferable, 15 months is a sufficiently long period to evolve the appropriate mesoscale detail in the boundary currents and gyres (which is not contained in the coarse-scale Levitus-based initialization). It is also long enough to allow NCEP forcing to produce conditions (e.g. SST and currents) appropriate to the hindcast year (Fig. 2). Buoyancy input for the Gulf of Alaska was derived from the analyses of Royer (1982 and personal communication), and is added at the surface of the water column along the coast in the CGOA. The weakly dissipative algorithms for tracer advection in ROMS obviate the need for strong explicit mixing; here, explicit Laplacian horizontal mixing coefficients were set at 50 m^2s^{-1} for momentum and 25 m^2s^{-1} for temperature and salinity.

ROMS includes algorithms for passive float tracking in three dimensions. Floats can be seeded at arbitrary locations and times, and re-seeded as required for the numerical experiment. Output includes Lagrangian time series of position, depth, salinity, temperature and density. We have utilized this feature to track the temperature history of passive particles during NEP runs, as an approximation to the life history of passive planktonic organisms (e.g. Pollock larvae).

A previous circulation model of the Southeast Bering Sea at 4 km resolution, with tidal and ice dynamics, has been reported in the literature (Hermann et al. 2002), but was not used here due to its limited domain size. In that model, an open boundary at the western edge of the domain required specification of the Aleutian North Slope Current, and the value chosen had a large impact on the internal dynamics. Since we have limited information about the interannual variation of this current (and hence the appropriate boundary value for each

hindcast year) we chose to use the NEP model, which generates its own ANSC based on the NCEP forcing for that year.

This figure is attached as NEPROMS SST FIGURE (PDF FILE from Al Hermann)

Figure 2. Model-generated sea surface temperature in the Southeastern Bering Sea for April 15, 2000. Axes denote latitude and longitude (degrees east). Bathymetry is contoured in meters. Note the penetration of warmer waters from the Gulf of Alaska through Unimak Pass.

References

Haidvogel, D. B., H. G. Arango, K. Hedstrom, A. Beckmann, P. Malanotte-Rizzoli, and A. F. Shchepetkin, 2000: Model Evaluation Experiments in the North Atlantic Basin: Simulations in Nonlinear Terrain-Following Coordinates, *Dyn. Atmos. Oceans*, **32**, 239-281.

Hermann, A. J., P. J. Stabeno. D. B. Haidvogel and D. L. Musgrave. 2002. A regional tidal/subtidal circulation model of the southeastern Bering Sea: Development, sensitivity analyses and hindcasting. *Deep-Sea Res. II: Topical Studies in Oceanography* (in press).

Marchesiello, P., J. C. McWilliams, and A. F. Shchepetkin, 2001: Open boundary conditions for long-term integration of regional oceanic models, *Ocean Modelling*, **3**, 1-20.

Royer, T.C., 1982. Coastal fresh water discharge in the Northeast Pacific. *J. Geophys. Res.*, **87**, 2,017-2,021.

Shchepetkin, A. F. and J. C. McWilliams, 1998: Quasi-monotone advection schemes based on explicit locally adaptive dissipation. *Mon. Weather Rev.*, **126,** 1541-1580.

3.7 ROMS Simulations Of Pollock EGG And Larvae Transport, by Dylan Righi.

Introduction: The North-eastern Pacific Regional Ocean Model System (NEPROMS) was used to simulate drifter trajectories in the southeastern Bering Sea. Drifter tracking in

ROMS is done using a fourth order predictor-corrector scheme. Drifters are allowed to move vertically. We currently have results for the years 1997-2001.

The simulated drifters are initialized over the eastern Bering Sea shelf just north of Unimak Island and to the northeast of Unimak Pass. This region is known to be an area of strong spawning for walleye pollock (*Theragra chalcogramma*). The initial drifter positions fill out a seven by seven grid with horizontal separations of about 10 kilometers (Figure 1). Vertically, there are 15 drifters initialized at each grid point with maximum depths just over 40 meters. The drifter initial positions are denser near the surface, replicating vertical egg distribution data collected in the Bering Sea (Kendall, 2001). Drifters are released on April 1 of each year and are tracked for 90 days.
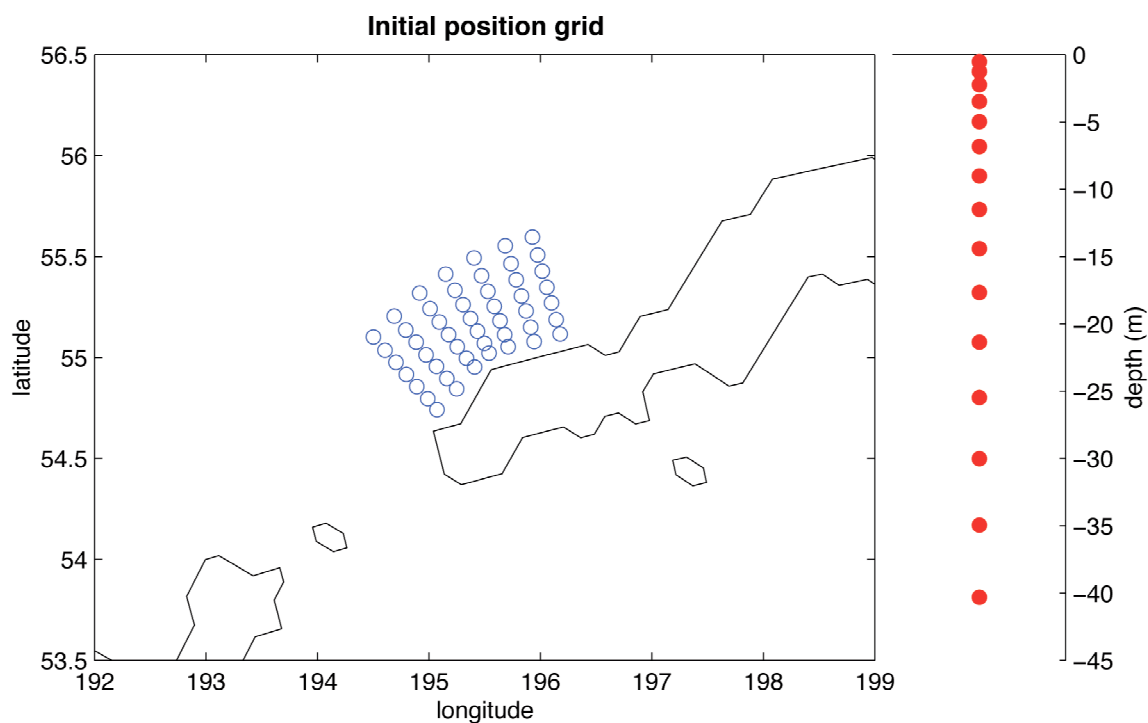

Figure 1. Simulated drifter initial horizontal (left) and vertical (right) positions.

Endpoints after 90 days for drifter trajectories from the 1997-2001 runs are shown in Fig. 2 (this plot shows all drifters at all depths). In all years there is a strong tendency for trajectories to move to the northeast up the Alaskan peninsula. The other common path is movement to the northwest along the 100-meter isobath. These patterns are qualitatively similar to circulation schematics that were constructed from current , satellite tracked drifter and hydrographic observations (e.g., Schumacher and Stabeno, 1998). The split between these two paths is seen clearly in the 1998, 1999 and 2001 drifter endpoints. In 1997 the full trajectory plots (not presented here) show that a subset of the drifters begin following the standard 100-meter isobath path, but then currents change and drive them up the shelf to the northeast. The endpoints in 2000 are the result of a strong turning to the northwest of

trajectories that had been moving up the Alaskan peninsula. Further study of possible
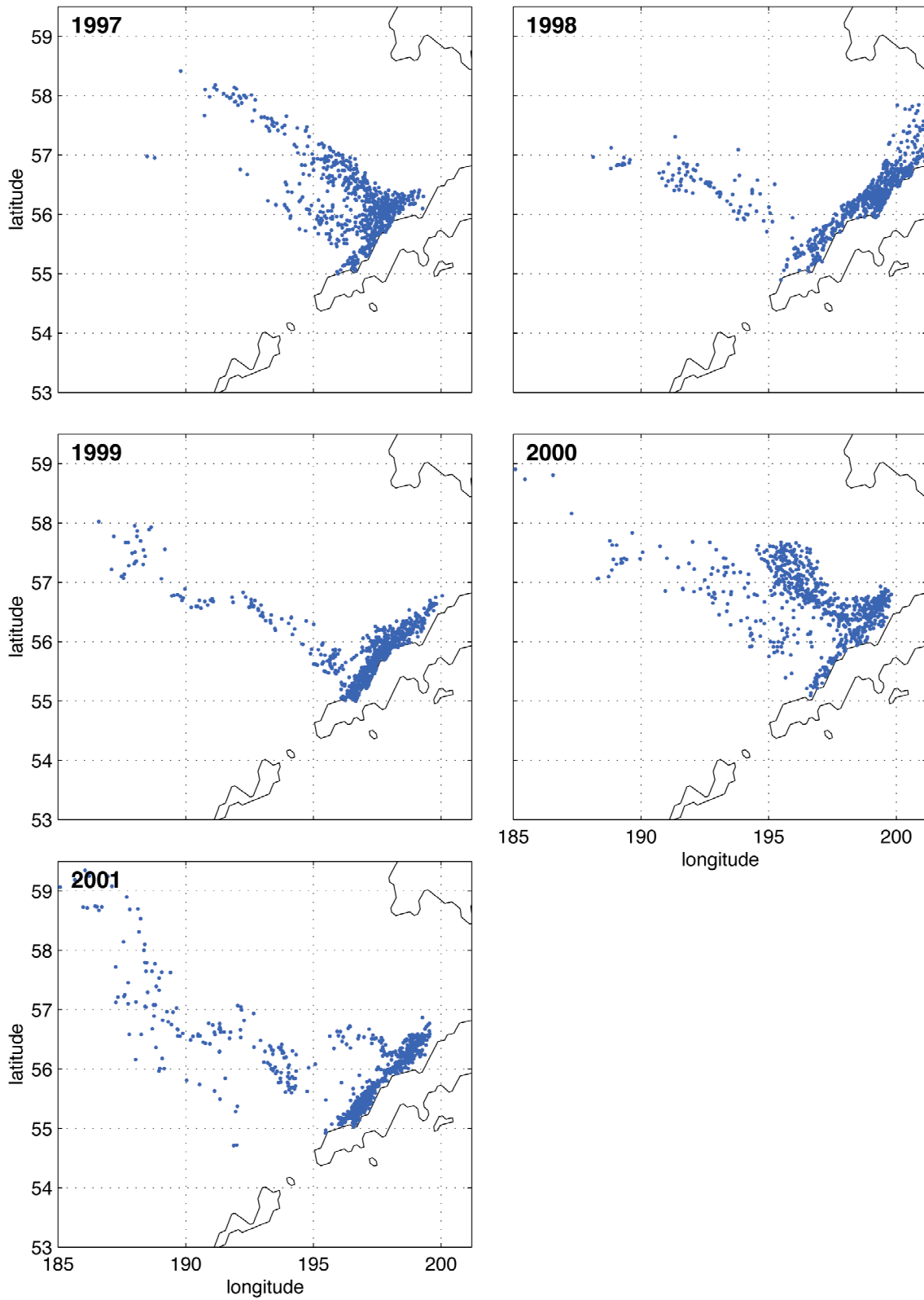

Figure 2 Endpoints for 90-day drifter trajectories for 1997-2001.

forcing mechanisms is needed to understand what leads to these years departing from the archetypal two-limbed flow.

The initial goal of this work was to compare simulated trajectories from a full primitive equation model with those from the Ocean Surface Current Simulations (OSCURS) numerical model. OSCURS computes daily surface current fields using daily sea level pressure and long-term mean geostrophic current data. As such, it is a simpler model in terms of the physics involved but is much more computationally inexpensive. Wespestad et.al., (2000) used OSCURS to create simulated trajectories in the Bering Sea. The initial grid used here was centered on the initial release point they used. Our trajectories for drifters released near the surface (0 to 5 meters depth) show good agreement with the OSCURS results. But our results show variation of trajectory endpoints with changes in both horizontal and vertical initial position. Figure 3 shows the full trajectories for the 2001 simulated drifters.
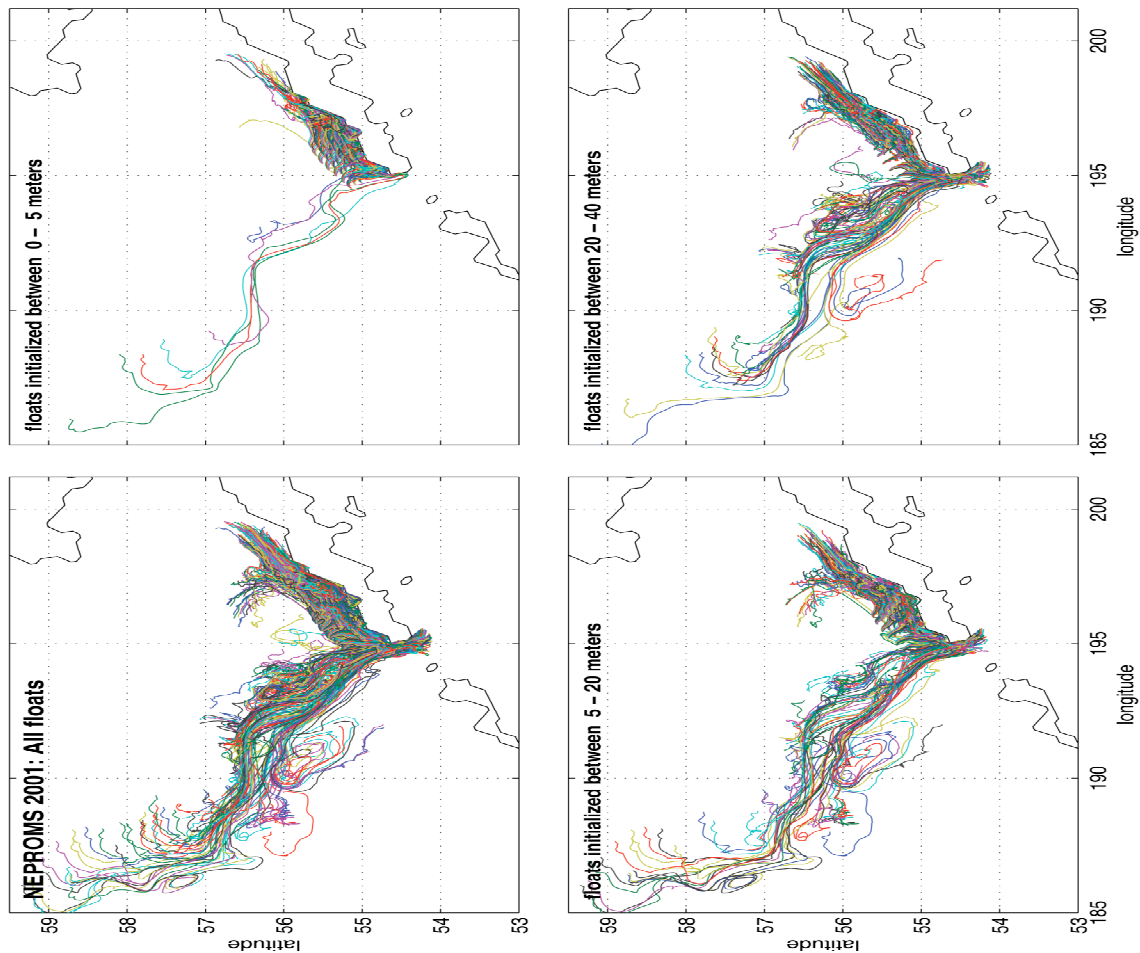

Figure 3 Full trajectories for the 2001 90-day simulated drifters. Lower left panel shows all drifters, while the other panels show drifters divided as a function of initial release depth.

The upper left panel shows the tracks of all the drifters released for the run. The upper right and the bottom panels show drifter tracks as a function of their release depth. The first facet of these plots is that there is a large dependence of where a drifter ends up on its initial horizontal placement.

The next point is that there is a strong dependence on release depth. The OSCURS 2001 trajectory moves a short distance to the northeast up the Alaskan peninsula as do the majority of the NEPROMS drifters released in the upper five meters of the water column (upper left panel of Fig. 3). But with deeper release points comes a stronger divergence of the trajectory fates. In the 5-20 meter and 20-40 meter release bins there are significant numbers of drifters that join the 100-meter isobath flow to the northwest, with some even moving through Unimak Pass before turning back. OSCURS results would completely miss this variation in particle fates.

References:
Kendall, Arthur W. Specific gravity and vertical distribution of walleye
pollock (Theragra chalcogramma) eggs. AFSC Processed Report 2001-01
January 2001, 45 pp.

Schumacher, J.D., and P. J. Stabeno, 1998. Continental shelf of the Bering Sea. *In*: The Sea: Vol. 11-*The Global Coastal Ocean: Regional Studies and Synthesis*, John Wiley & Sons, Inc, New York, NY, 789-822.

Wespestad, V.G., L.W. Fritz, W.J. Ingraham, Jr., and B.A. Megrey, 2000. On relationships between cannibalism, climate variability, physical transport and recruitment success of Bering Sea walleye pollock, *Theragra chalcogramma. ICES J. Mar. Sci. 57:* 272-278.

4. APPLICATION OF A TRANSPORT AND PREDATION INDEX TO RECRUITMENT FOR STOCK ASSESSMENT PURPOSES by Jim Ianelli

Background

Recruitment or year-class strength (the numbers of fish successfully surviving larval and post-larval stages, e.g., to age 1) is a fundamental part of the population model used for pollock stock assessments (e.g., Ianelli et al., 1998). The recruitment estimates provide the basis for population numbers that are tracked over time and modified by various natural and fishing mortality sources. The statistical assessment models used in these analyses are similar to state-space models where unknown and unobservable quantities (e.g., numbers of

fish) are modeled separately as "state" variables. "Observation" equations are then constructed to translate the state variables into model predictions. These predictions are then compared with actual data to tune the state variables (i.e., the fundamental parameters) using statistical methods such as maximum likelihood. Schnute (1994) provides a good description of this general approach.

Estimates of year-class strengths (e.g., Fig. 1) are thus derived from a variety of information used in the assessment model. This information includes annual bottom-trawl surveys of the entire shelf area (within the US EEZ), bi-annual echo-integration trawl (EIT) surveys of this region, annual fishery catch data from scientific observers aboard fishing vessels, and estimates of biological characteristics (e.g., age composition, growth, and maturation). These assessment analyses lead to recommendations on risk-averse harvest levels for the coming year. The recommendations are influenced by estimates of the underlying stock-recruitment relationship within the integrated assessment model (the so-called stock-recruitment sub-model; Fig. 2). Further, the stock-recruitment sub-model can be modified to incorporate environmental indices. Since the framework of the integrated model separates the state dynamics from the observations, it is relatively straightforward to test alternative hypotheses. We illustrate one such modification to evaluate the impact of progressively adding recruitment effects beginning with the simplest form (a mean and deviation) and then additional terms related to the stock size and any environmental terms and process errors. These can be written as recruitment state variables:

$$1) \quad R = Mean + \varepsilon$$

$$2) \quad R = f(S) + \varepsilon$$

$$3) \quad R = f(S) + E$$

$$4) \quad R = f(S) + E + \varepsilon$$

$$5) \quad R = f(S) + E' + \varepsilon$$

where R is actual (unobserved) state variable (log-recruitment) for a given year and the error term (ε) can be thought of as one that encompasses all "natural" variability that is not described by other terms in the above sub-models. For example, sub-model 3) is written such that all recruitment variability is determined by the stock-recruitment function (denoted $f(S)$) and an environment term (E). This simply means that the there is no residual process error in recruitment specifications (i.e., the model terms determine all of the variability in recruitment. For Model 5, the conditions for the environment term (E', described below) are "smoothed" with respect to spatial correlation.

In searching for the appropriate environmental term(s), water temperature, turbulence and transport have been related to success of recruitment for many marine species (e.g., Quinn and Niebauer 1995). Here, we follow the construct that the transport of planktonic stages is important to establish separation of young pollock from their cannibalistic adults

(Wespestad et al. 2000). We used the Ocean Surface Current Simulations (OSCURS) numerical model (Ingraham and Miyahara, 1988) as a means to represent the effective inter-annual variability of advective egg and larval transport.

An application

The following serves to illustrate one method for incorporating environmental information within an integrated stock assessment approach such as that currently used for EBS pollock. Incorporation of any index can be done in a similar fashion. The integrated assessment model is a good way to evaluate candidate indices because consistency with all available data can be easily evaluated. In addition, compared to methods simply using recruitment residuals, the integrated model provides a more statistically defensible approach since fewer assumptions are required (e.g., analyses of residuals done separately typically fail to account for the uncertainty of the estimates of the residuals themselves). A disadvantage of the integrated assessment approach is that a fair amount of specialization is required to run the models.

The OSCURS model was run from a single launch site (55.5 N, 165 W) for 90 d trajectories starting April 1. This location and date was selected based on the distribution and timing of the main concentrations of spawning pollock. The variability of this location appears to be moderate based on the catch-distribution of the fishery for pre-spawning pollock (Fig. 3). However, this observed variability is partly attributed to fleet behavior under variable ice conditions and management measures.

Simulations were generated for the years 1964 to 1998 (Fig. 4). The endpoints of these trajectories suggest that the young-of-year pollock are either just seaward of the inner front or in the coastal domain as defined in Kachel et al (in press). To quantify the effect these trajectories may have on recruitment success, we chose to compute the average location of the 90-day drifter. The average location represents the characteristics of the advective forces better than the endpoints and reduces the impact of drift outliers (i.e., high-levels of drift over a few days). These average locations were then placed in the context of a grid (Fig. 5) in order to geo-reference the advection by year. Each year was therefore assigned to a grid- cell (but not all grid-cells had observations). The integrated assessment model was then used to estimate the "effect" a particular grid-cell has relative to recruitment success. In other words, each cell was estimated as being favorable, unfavorable, or neutral to pollock year-class strength.

To make the model well conditioned, two penalty weights were added to the (negative-log) likelihood function. First, a very small grid-cell penalty was added so that for cells with no observations, the estimated recruitment effect would be nil (yet still with the desired high variance). The second (more important) penalty effectively conditions the grid surface values to have a non-parametric surface such that there is some degree of spatial correlation. The value of this penalty weight affects the "smoothness" of the surface by way of multiplying the sums of squared third-differences between grid-cell values in both the lateral and longitudinal directions (Ianelli 1998). In the limit, as the value of this multiplier becomes large the effect of the grid on explaining recruitment variability goes to zero (i.e., the two-dimensional surface is represented a single mean value). As the smoothness penalty multiplier tends towards zero, the cells become independent from contiguous (and all other)

cells. Alternative values of this multiplier have been explored and are shown if Figs. 6a and 6b. Note that in Fig. 6a the "effect" of larval drift is more irregular compared to the model where smoothness in space is assumed (Fig. 6b).

Table 1. Root-mean squared errors of recruitment sub-model results.

Model component	Model 1	Model 2	Model 3	Model 4	Model 5
Mean	0.00	-	-	-	-
Stock-recruitment function, $f(S)$	-	0.04	0.08	0.09	0.09
OSCURS avg. drift	-	-	0.48	0.21	0.11
Residual (ε)	0.75	0.72	-	0.21	0.28
Total	0.75	0.75	0.56	0.51	0.47

Discussion

For the Eastern Bering Sea, wind-driven advection of surface waters containing planktonic stages of pollock (Wespestad *et al.*, 2000) and Tanner crabs (Rosenkranz *et al.,* 2001) appears to account for some of the observed fluctuations in year-class strength. In these studies the biological process that links advection to year-class strength is differential survival.

The role of cannibalism in influencing population dynamics resulting from the strong year class has been examined (Livingston and Methot, 1998). For the age – 0 pollock, predation by older pollock can have a strong influence on year – class strength.

A number of caveats exist in the above analysis. For example, the mechanistic model is one that deals with the negative effects of spatial overlap between age 1 juveniles with pollock that are generally older than age 2 (Fig. 7). Analyses of an index of separation (Eq. 1) may provide some insight on whether other data are consistent with this process.

$$\sqrt{ p} \quad 2$$

1)
$$\frac{}{\sqrt{}}.$$

where p_{age1} and p_{age2+} are the proportions at age 1 and ages 2 and older, respectively. These values were computed at each of at a given survey site and the number of stations in sampled in the standard area (Wespestad et al, 2000). Results compared with log-recruitment suggest a very weak relationship between separation index and year-class strength (Fig. 8).

Another caveat from this approach is that there are physical and biological assumptions imbedded in how accurately OSCURS simulates the actual transport of pollock eggs/larvae. From a purely physical perspective we accept that OSCURS is a surface wind – drift model most applicable to approximately the upper 10 m of the water column and to regions where the ambient subtidal currents are weak. For much of the southeastern shelf the

climatological mean currents are weak yet more active flow has been observed along the 100 – m isobath and over the outer shelf/slope (Schumacher and Stabeno, 1998, Reed and Stabeno, 1996, Reed, 1999, Stabeno et al., 2001).   One solution is to compare the results from OSCURS to those from more sophisticated hydrodynamic models.   Early indications suggest that there is good agreement except in areas where depth dynamics are particularly acute, e.g., around the Pribilof Islands.

From a purely biological perspective the question of location of planktonic stages in the water column, and selection of a single launch site must be examined. We show some indication of inter-annual variability of spawning location (Fig. 3) that may be useful to improve launch-site locations. Additionally, multiple launch sites in space and time may also better represent the effect of advection on pollock eggs and larvae. While extensive work has not be conducted on the vertical location of eggs and larvae, over the shelf larvae do exist in the upper 10 m, but they often found at greater depths (Napp et al, 2000). This raises the question on what fraction of the planktonic life history stages would follow the wind-drift.

Spawning also occurs near Bogoslof Island and other locations over the slope/basin of the eastern Bering Sea. These regions were hypothesized to be a source of larvae for the southeastern shelf (Francis and Bailey, 1983). If significant spawning occurs off the shelf where high concentrations of larvae have been observed (Schumacher and Stabeno, 1994), then the simple set of initial conditions for the drift-effect on recruitment are further complicated. It appears that larvae in these waters are likely to be deeper in the water column (Napp et al, 2000) and the background currents are typically stronger than over the middle shelf (Stabeno et al, 1999).   Alternative drift locations to represent the starting points of egg and larval stages may require further exploration, particularly if there is a significant amount of pollock egg production from the Aleutian basin region.

References

Francis, R.C. and K.M. Bailey, 1983. Factors affecting recruitment of selected gadiods in the northeastern Pacific and east Bering Sea. *In:* Year to Year Interannual Variability of the Environment and Fisheries of the Gulf of Alaska and the Eastern Bering Sea. Pp. 17-22, Ed. By W. S. Wooster, Washington Sea Grant, University of Washington, Seattle, WA, USA.

Ianelli, J., L.W. Fritz, T. Honkalehto, N. Williamson and G. Walters. 1998. Eastern Bering Sea walleye pollock stock assessment with yield considerations for 1999. *In:* Stock Assessment and Fishery Evaluation Report for the Groundfish Resources of the Bering Sea/Aleutian Islands Regions, pp. 31-111. Ed by Groundfish Plan Team for the Bering Sea-Aleutian Islands Region, North Pacific Fishery Management Council, 605 W 4th Ave., Suite 306, Anchorage, AK. 99501. 560 pp.

Ianelli, J.N., T. Buckley, T. Honkalehto, N. Williamson and G. Walters. 2001. Bering Sea-Aleutian Islands Walleye Pollock Assessment for 2002. *In*: Stock assessment and fishery evaluation report for the groundfish resources of the Bering Sea/Aleutian Islands regions. North Pac. Fish. Mgmt. Council, Anchorage, AK, section 1:1-105.

Ingraham, W.J. Jr. and R.K. Miyahara, 1988. Ocean surface current simulations in the North Pacific Ocean and Bering Sea (OSCURS-Numerical Model). US Department of Commerce, National Oceanic and Atmospheric Administration, Technical Memorandum, National Marine Fisheries Service F/NWC-130. 155 pp.

Kachel, N. B., S. A. Salo, J. D. Schumacher, P. J. Stabeno and T. E. Whitledge, in press. Characteristics of the Inner Front of the Southeastern Bering Sea*. Deep Sea Res., Topical Studies in Oceanogr.*

Livingston, P.A., and R.D. Methot, 1998. Incorporation of predation into a population assessment model of eastern Bering Sea walleye pollock. *In*: Fishery Stock Assessment Models, Alaska Sea Grant College Program, AK-SG-98-01: 16 pp.

Napp, J.M., A.W. Kendall, Jr., and J.D. Schumacher, 2000. A synthesis of biological and physical processes affecting the feeding environment of larval walleye pollock (*Theragra chalcogramma)* in the eastern Bering Sea. *Fish. Oceanogr. 9*:147-162

Quinn, T.J. II. and H.J. Niebauer. 1995.   Relation of eastern Bering Sea walleye pollock (*Theragra chalcogramma*) recruitment to environmental and oceanographic variables. In: R.J. Beamish (Ed) Climate Change and Northern Fish Populations. Can. Spec. Publ. Fish. Aquat. Sci. 121:497-507.

Reed, R.K. and P.J. Stabeno, 1996. On the climatological mean circulation over the eastern Bering Sea shelf. Cont. Shelf. Res., 16(10), 1297–1305.

Reed, R.K., 1999. A time series of temperature, salinity, and geopotential across the southeastern Bering Sea shelf, 1995–1999. NOAA Tech. Report ERL 455-PMEL 43 (NTIS PB2000-100564), 15 pp.

Rosenkranz, G.E., A.V. Tyler and G.H. Kruse, 2001. Effects of water temperature and wind on year - class strength of Tanner crabs in Bristol Bay, Alaska. *Fish. Oceanogr. 10, 1:* 1-12.

Schnute, J.T. 1994. A general framework for developing sequential fisheries models. Can. J. Fish. Aquat. Sci. 51: 1676-1688.

Schumacher, J.D., and P. J. Stabeno, 1998. Continental shelf of the Bering Sea. *In*: The Sea: Vol. 11-The Global Coastal Ocean: Regional Studies and Synthesis, John Wiley &Sons, Inc, New York, NY, 789-822.

Schumacher, J.D., and P.J. Stabeno, 1994. Ubiquitous eddies of the eastern Bering Sea and their coincidence with concentrations of larval pollock. *Fish. Oceanogr. 3*, 182–190.

Stabeno, P.J., J.D. Schumacher, and K. Ohtani, 1999.   Physical oceanography of the Bering Sea. *In*: Loughlin, T. R., and K. Ohtani (eds.), Dynamics of The Bering Sea: Physical, Alaska Sea Grant College Program, Fairbanks, AK. 1-28.

Stabeno, P.J., N. A. Bond, N. B. Kachel, S. A. Salo, and J. D. Schumacher, 2001. Temporal Variability in the Physical Environment over the Southeastern Bering Sea. *Fish. Oceanogr. 10*: 81-98.

Tyler, A.V and A.B. Hollowed, 2001. Groundfish trends in the eastern Bering Sea. Prepared for the SEBSCC Synthesis Group, pp. 11.

Wespestad, V.G., L.W. Fritz, W.J. Ingraham, Jr., and B.A. Megrey, 2000. On relationships between cannibalism, climate variability, physical transport and recruitment success of Bering Sea walleye pollock, *Theragra chalcogramma. ICES J. Mar. Sci. 57:* 272-278.
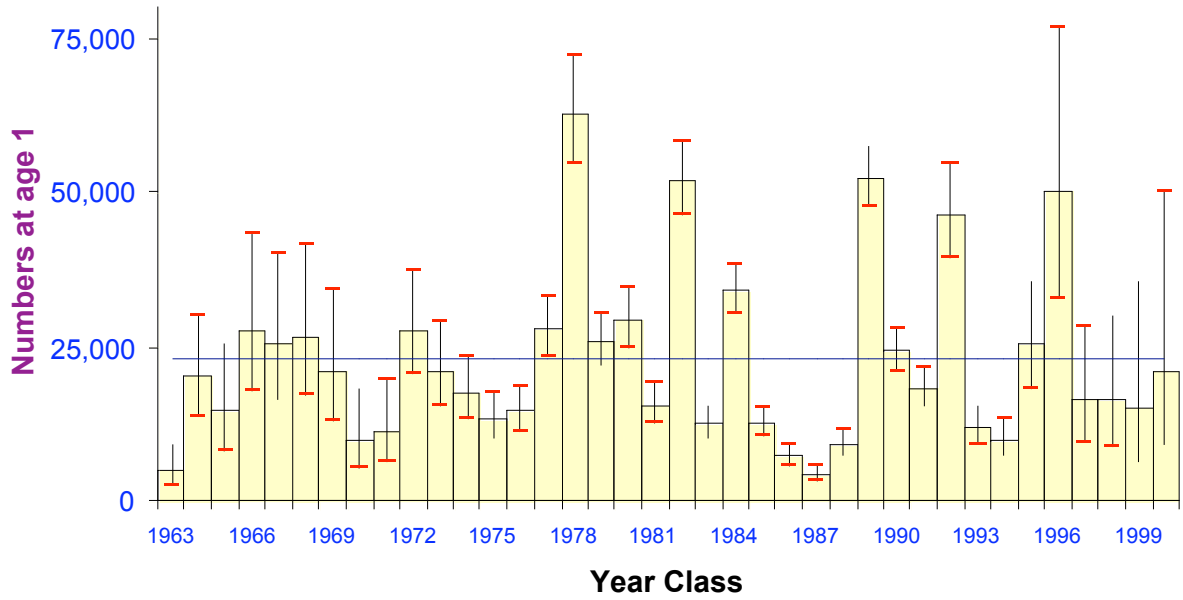
Figure 1.   Time series of year class abundance at age 1. Error bars represent approximate 95% univariate confidence bounds. Note that covariance estimates among adjacent year-classes is typically highly negatively correlated. Source: Ianelli et al. 2001.
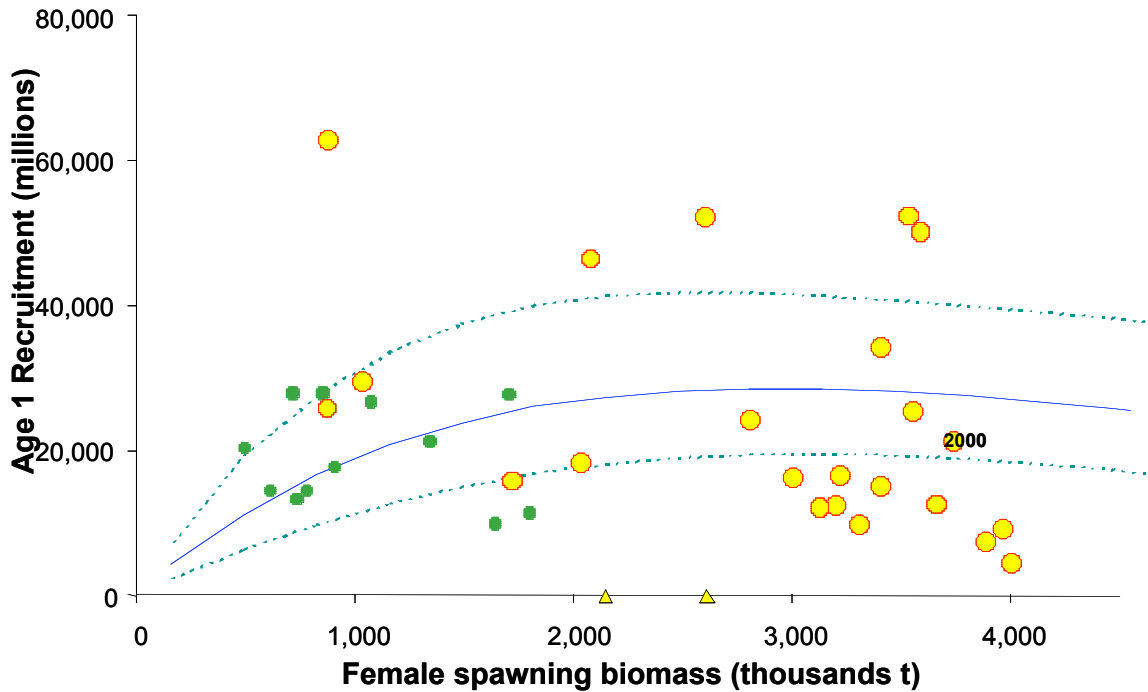

Figure 2.   Stock-recruitment relationship showing the fitted effect due to spawning biomass (thick line) and estimates from the stock assessment model. Note that the large dots are used to tune the stock-recruitment sub-model while the smaller dots represent points from the regime prior to 1977. Dashed lines represent approximate 95% confidence bands about the curve. Source: Ianelli et al. 2001.
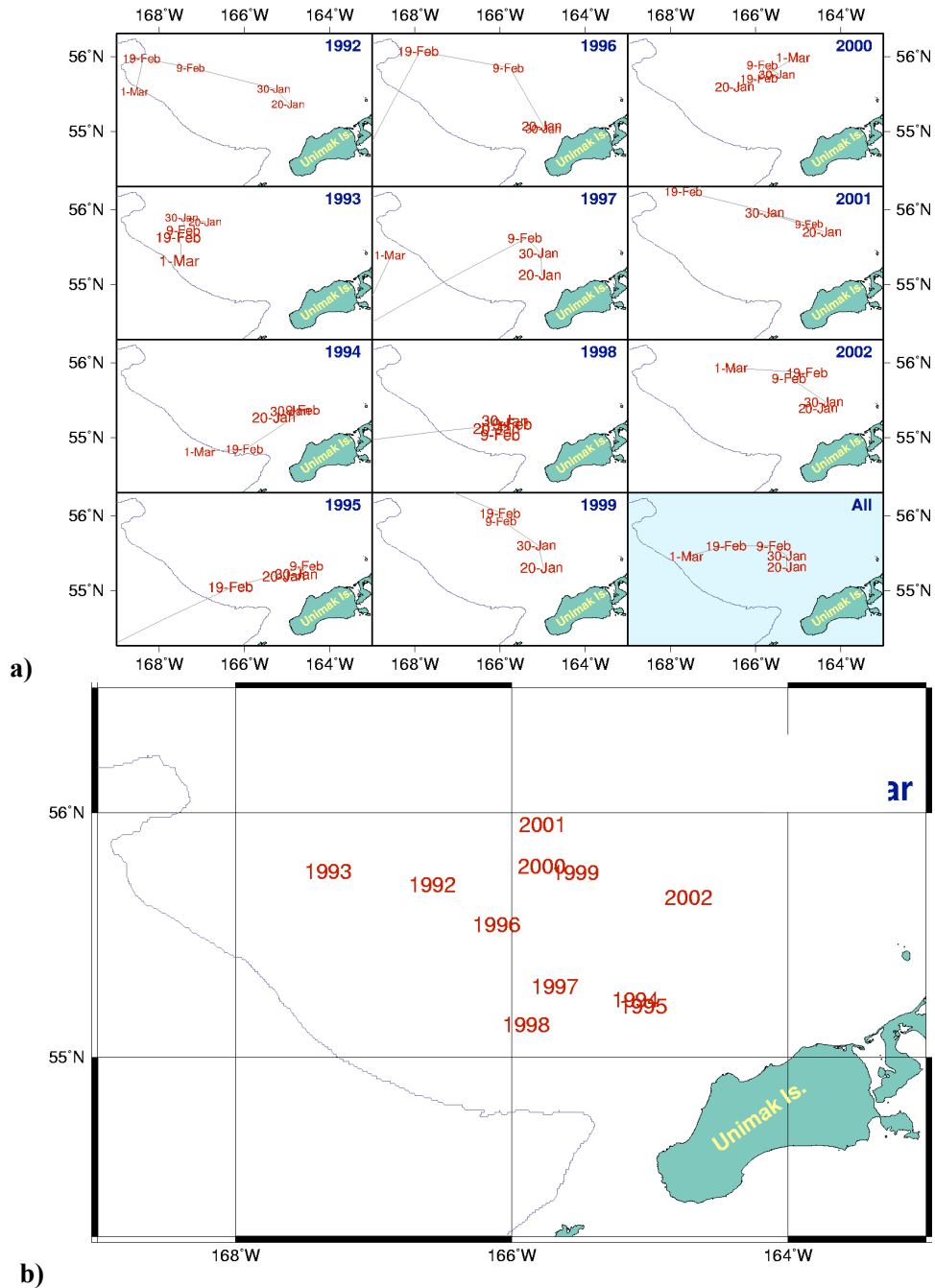
Figure 3. **Top panel a):** Average catch distribution by 10-day periods, 1992-2002. Bottom right corner is average over all years combined.
Bottom panel b): Average catch distribution of the pollock fleet targeting pre-spawning pollock by year, Jan 20th – Feb 28th.
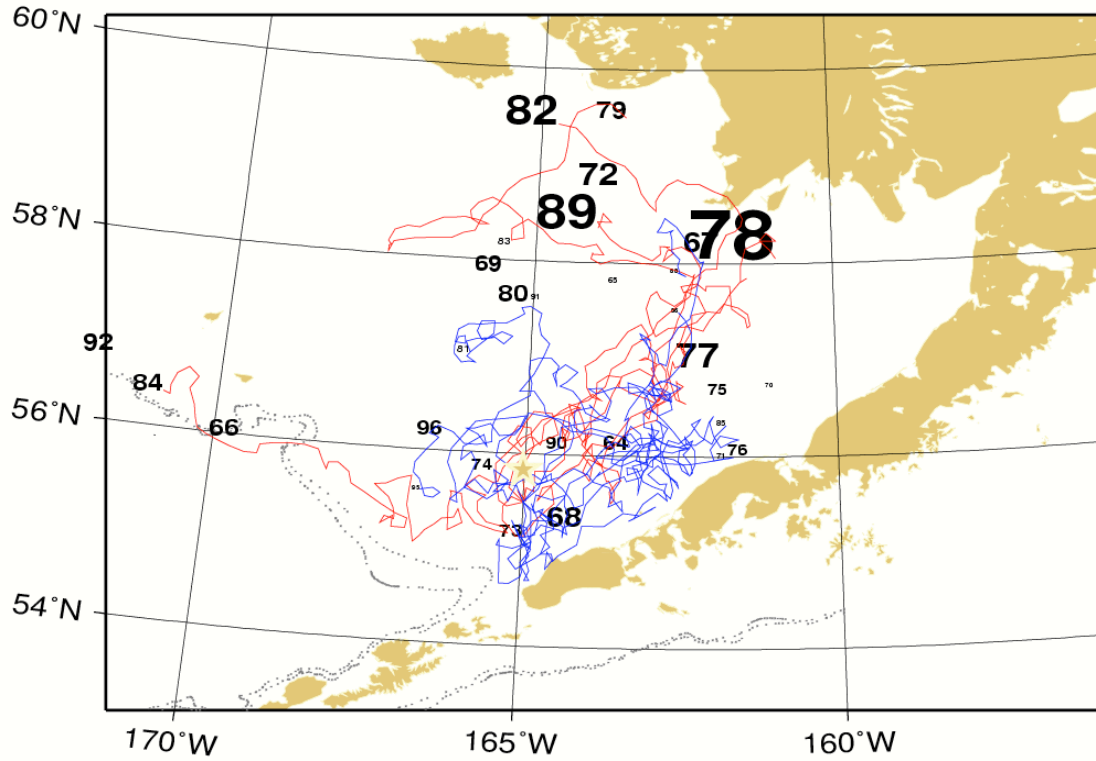
Figure 4.   Trajectories resulting from 90 day simulated wind drift from the initial launch site (annotated with a star). The size of the labeled year indicates the relative strength of that year class.
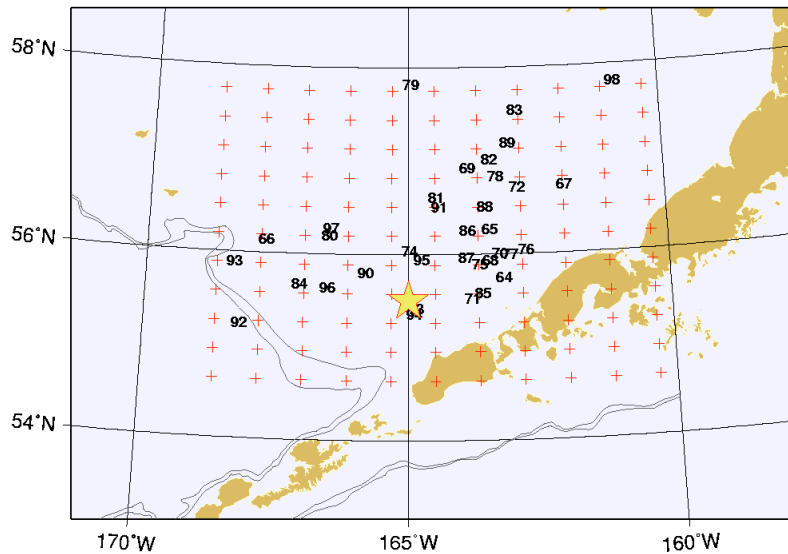

Figure 5.   Arbitrary grid locations (crosses) and average location of 90-day simulated drifters (begun at the star from April 1st) indicated by two-digit year (number).
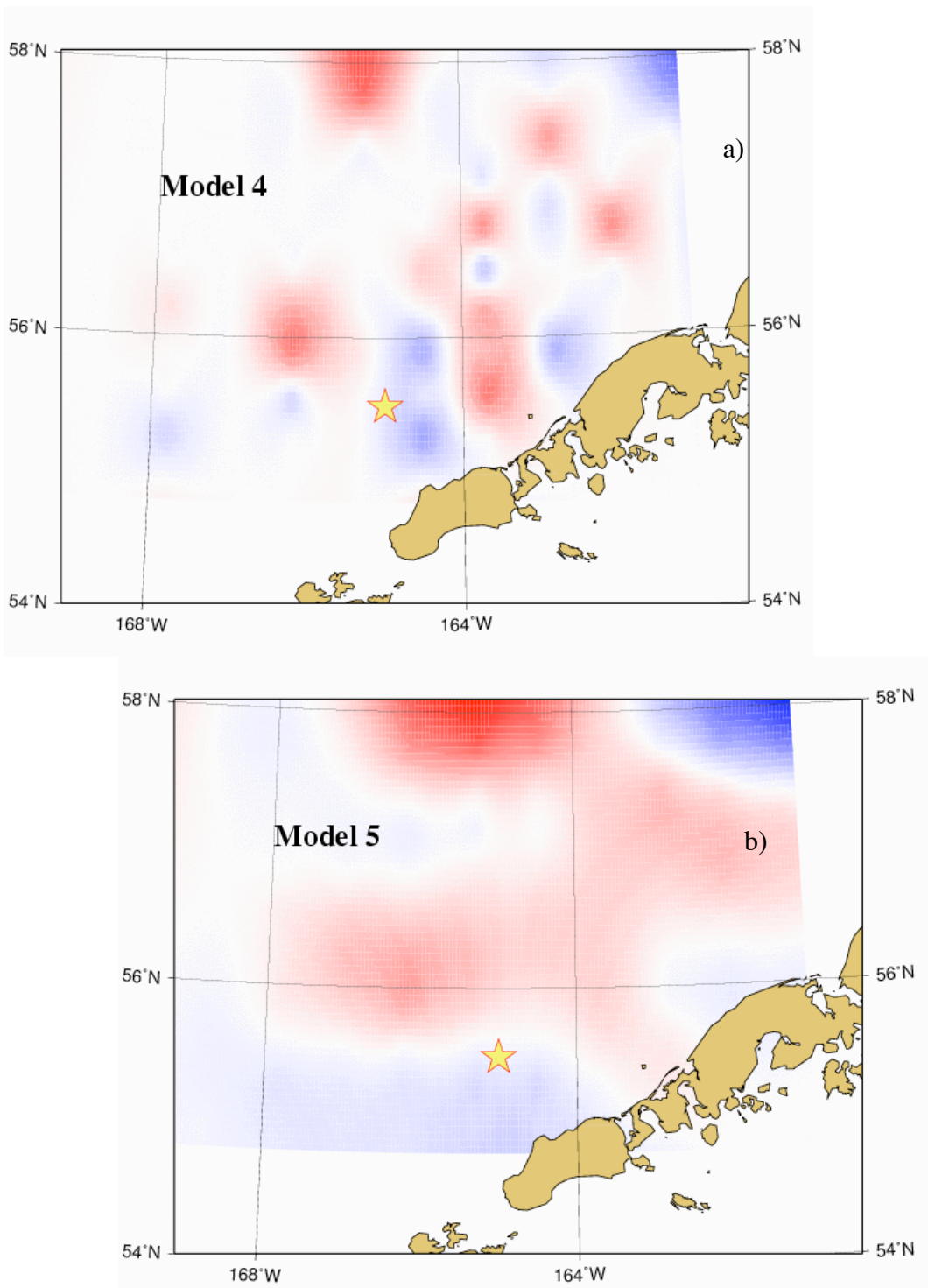
Figure 6.   Graphical results of fitting a drift component within the integrated stock assessment model. Red areas indicate higher recruitment success while blue represents lower values. Panel a) is the result for Model 4 (not smoothed) compared with Model 5 (where some degree of spatial correlation is specified).

Figure 7.   Length of pollock consumed compared to the length of the consuming pollock based on NMFS food-habits studies (Troy Buckley, pers. comm.).

Figure 8.   Separation index relative to estimates of the log-pollock abundance at age 1, 1982-1999. Numbers plotted represent year-class.

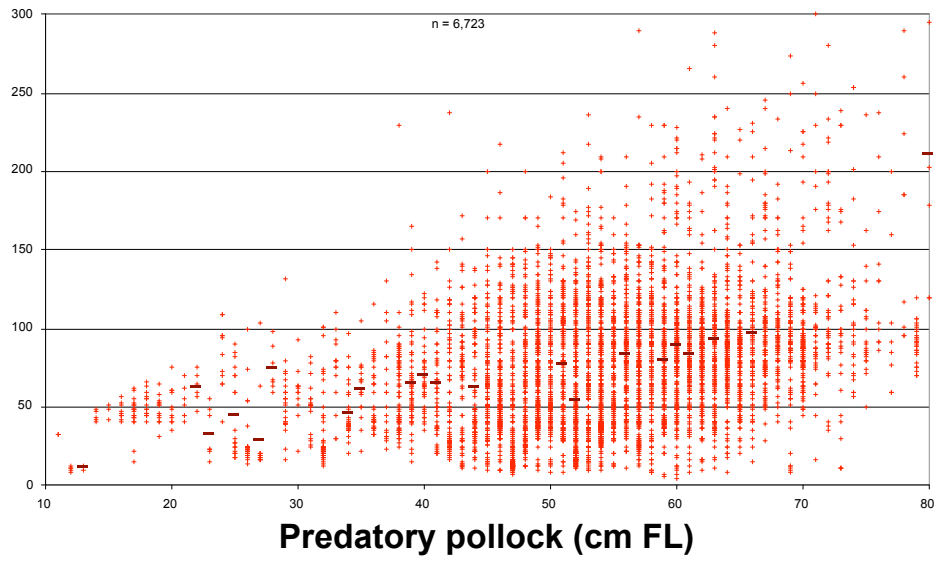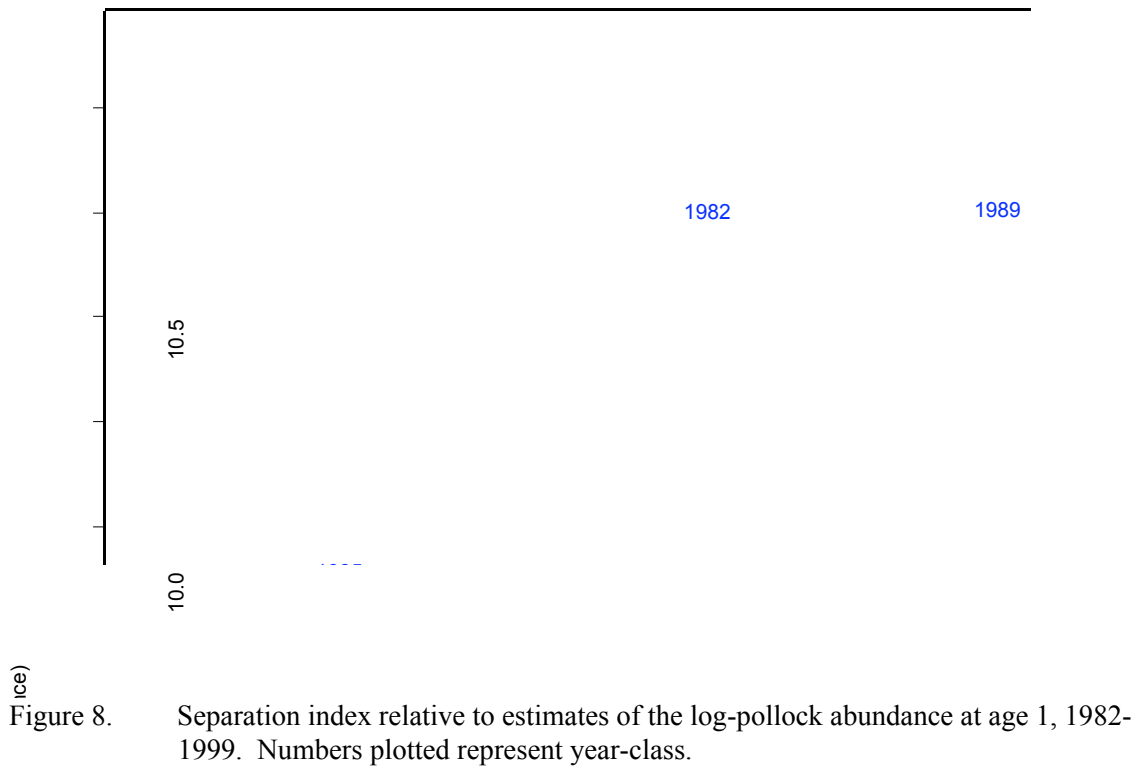## 5. CHANGING RELATIONSHIPS BETWEEN CLIMATE AND BIOLOGICAL INDICES IN THE EASTERN BERING SEA by Alan Springer

Introduction

Climate change, whether considered at local or global spatial scales and annual or millennial time scales, is among the most controversial and intriguing environmental issues confronting us today. The obvious concerns over climate change are effects it has on ecosystem structure and function, food web productivity, the abundance of individual species, and the economies and livelihoods of people the world over.

Nowhere have the effects of climate change on marine ecosystems been more well-documented than in the N. Pacific (e.g., McGowan 1990; Ebbesmeyer et al. 1991; Beamish 1995; Mantua et al. 1997; Francis et al. 1998; Klyashtorin and Rukhlov 1998; Springer 1998; Welch et al. 1998; Anderson and Piatt 1999; Hare et al. 1999; Hare and Mantua 2000). The common approach in most analyses of climate and other ecosystem components has been to compare slopes of parameter values over time, slopes that change when the climate changes from one quasi-stable state, or regime, to another. Regime shifts are defined by abrupt, sustained polarity reversals of the Pacific Decadal Oscillation (PDO) (Trenberth and Hurrell 1994; Mantua et al. 1997).

In contrast, there have been comparatively few analyses of relationships between two variables when time was not one of them. In order to better understand ecosystem processes that respond to climate change and regime shifts, it would be helpful to have correlations between things that are, or might be, functionally related. For example, correlations between fluctuations in primary physical forcing parameters, such as the Aleutian Low pressure field, and some response variables, such as wind, mixing depth, and primary productivity, as was modeled for the Gulf of Alaska by Polovina et al. (1995); and temperature and zooplankton population dynamics in the Gulf of Alaska (Mackas et al.,1998).

A small assortment of data sets for the Bering Sea can be grouped in ways that yield marginally miscellaneous and eclectic, but compelling, relationships. These relationships provide insight into time/space scales of interest and the sensitivity of ecosystem components and processes to climate change. This includes changes in the general climate state, *sensu* PDO, and to interannual fluctuations in climate within and across regimes.

Some of the relationships are between adjacent ecosystem elements that could be thought of as functional cause and effect relationships. Other relationships are separated by more than one element. Such ostensibly functional relationships are useful to know, even if the variables are separated by more than one trophic level, since they may give clues about where and how to look for processes responsible for biomass yield at any trophic level.

Observations

The time series used to develop and examine potential relationships are:

1   North Pacific Index (NPI) – area averaged mean sea level pressure anomaly over the region 30º to 65ºN, 160ºE to 140ºW (Trenberth and Hurrell 1994, Minobe, 1999)

2   Sea surface temperature (SST) – mean temperature of a 5º x 5º block centered on 55ºN, 170ºW (D. Cayan unpubl. data)

3   Bering Sea wind measured at St. Paul I. by the U.S. Weather Service Note, the wind speed has been cubed so that it provides an index of mixing.

4   Sea ice – coverage over the eastern Bering-Chukchi shelf (Niebauer 1998, unpubl. data)

5   Bering Strait transport – annual northward transport through Bering Strait (Roach et al. 1995, T. Weingartner unpubl. data)

6   Global ocean temperature (>>>)

7   Bowhead whale baleen stable carbon isotope ratios ($\partial^{13}C$) (Schell 2000)

8   Steller sea lion abundance (NMML 1994, unpubl. data; Trites and Larkin 1996)

9   Age 1 pollock abundance and age 3+ pollock biomass (J. Ianelli unpubl data)

10   Red-legged kittiwake productivity at St. George I., Pribilof Is. (Dragoo et al. 2001)

11   Seabird abundance at the Pribilof Is. and Aleutian Is. (Dragoo et al. 2001)

12   Fur seal pup production on St. Paul I., Pribilof Is. (York and Hartley 1981; York and Kozloff 1987, A. York unpubl. data)

13   Fur seal growth rates (A. Trites unpubl. data)

14   Common murre and thick-billed murres relative abundance at Walrus I., Pribilof Is. (Peterson and Fisher 1955).

Physical-physical Relationships

Despite considerable uncertainty about the relative importance of processes governing community structure and the abundances of individual species, e.g., top-down versus bottom-up interactions, much that transpires in ecosystems begins with physics. Francis et al (1998) have presented a conceptual model of the pathways by which changes in atmospheric features can influence biota, and Schumacher et al (in press) have modified this model for the Bering Sea. Both of these models show that physics can influence an ecosystem in either top dow or bottom up modes. For the North Pacific and eastern Bering Sea, much of the physics begins with the Aleutian Low pressure system that can be scaled by the North Pacific Index (NPI).

Winter sea ice extent and duration in the Bering Sea are related at the decadal scale to mean atmospheric forcing (Niebauer 1998; Wyllie-Echeverria and Wooster 1998; Stabeno et al., 2001). Sea ice influences the ecosystem through at least two pathways. First, the presence of sea over the southeastern shelf in March (when ambient light is adequate to sustain primary production) can result in an early phytoplankton bloom. An early bloom may result in a greater energy flow to the benthic community, whereas a bloom later in spring likely favors pelagic pathways. The extent of sea ice is also vital to the subsequent development of the middle shelf cold pool that appears to influence the distribution of pollock and Arctic cod. The timing and magnitude of the summer retreat of sea ice is related to summer climate, which can be indexed by the NPI (Figure 1). Recent results indicate that regions of the Bering Sea have shifted toward an earlier spring transition (Stabeno and Overland, 2001). The retreat/melting of sea ice also has ecosystem effects as it alters the availability and distribution of essential habitat for symphagic food webs and pagophilic marine mammals and is related to energy flow through the ecosystem as noted above.

One of the hallmark features of the Bering Sea is the transport of water north through Bering Strait into the Chukchi Sea. This transport occurs because of differential atmospheric pressure across the Western Arctic that tilts sea level down toward the north (Coachman et al. 1975). Not surprisingly, then, variability in annual transport is related to variability in atmospheric pressure, as reflected again by the NPI (Figure 2). A long-term decline in the mean strength of the Aleutian Low may explain the decline in transport in the

past 5 decades. This in turn would be expected to have a large effect on production budgets across the northern Bering-Chukchi shelf, since nutrients and biota carried in the current transform the region into one of the most highly productive regions in the world (Springer et al. 1989; Springer and McRoy 1993).

Wind measured at St. Paul I. is related to the atmospheric pressure field (Figure 3). The dramatic drop in the mean winds during the mid-1970s to late 1980s corresponded to a similar change in the NPI and to a pronounced increase in average global ocean temperature (Figure 4).

St. Paul wind is also related to ocean temperature in the Bering Sea (Figure 5). However, the correlation is only apparent within a given regime and changes from one regime to the next. That is, wind and SST were generally out of phase prior to 1977, were generally in phase between 1977 and 1989, and then generally out of phase again after 1989. Interannual fluctuations in wind and SST are not always proportional, indicating, not surprisingly, that other factors are important in determining magnitudes of the two variables.

Physical-biological Relationships

Carbon stable isotope ratios ($\partial^{13}C$) of baleen from bowhead whales exhibit considerable interannual variation since the late 1940s, including a pronounced overall shift that has been proposed as evidence of a decline in primary productivity of some 30% in the Bering Sea (Schell 2000). The pattern in baleen $\partial^{13}C$ variability matches the pattern in winds over the same interval when baleen is lagged by 1 year to account for the ecological distance [define] between whales and physical forcing (Figure 6).

Wind also is correlated in a general way with sea lion abundance at sweveral colonies in the Bering Sea range of the endangered western stock (Figure 7). That is, sea lion abundance declined abruptly and precipitously at the same time that winds declined in a similar manner in the Bering Sea.

Sea surface temperature (SST) has varied since the late 1940s and is highly correlated with at least four biological variables in the Bering Sea—the abundance of age 1 pollock, the biomass of age 3+ pollock, and the productivity of black-legged and red-legged kittiwakes on the Pribilofs. However, except for age 3+ pollock biomass, the correlations exist only within regimes as defined by the PDO, where they are very strong but have

alternating signs from regime to regime (Figures 8, 9). Pollock biomass was positively correlated with spring SST for 25 years when SST is lagged by 4 years to account for separation between given SST years and the integrated effect expressed in the pollock age classes where most biomass resides (Figure 10). Does the 4-year lag also suggest that most of the impact of SST (or whatever it is surrogate for) on pollock populations occurs between egg and age-0 fish? If so, there are many possible pathways one could infer from the correlation.

Biological-biological Relationships

The most conspicuous correlations between biological variables in the Bering Sea are trends in abundances of piscivorous seabirds and fur seals on St. Paul I. and St. George I. (Pribilof Is.) and Bogoslof I. and Buldir I. in the Aleutian Is. (Table 1). Trends are uniformly negative on St. Paul and uniformly positive on Bogoslof and Buldir. On St. George, both species of kittiwake and fur seals are declining as at St. Paul: thick-billed murres declined through the 1980s but have increased since then, whereas common murres increased throughout this period. All of these species are supported by a common suite of pelagic forage fishes and squids that includes prominently juvenile pollock at the Pribilofs.

There is an obvious similarity between the pattern of change in fur seal numbers at St. Paul—a prolonged decline punctuated by intervals of increase—and the pattern of change in $\partial^{13}C$ of bowhead whale baleen (Figure 11). Were it not for the overriding effect of the female harvest on population stability in the period 1956-1968 (York and Hartley 1981), the response of fur seals to an apparent environmental signal might have been stronger. That is, the increasing trend in numbers in the mid-1960s may have been attenuated by pressure on the population from excessive female harvests. Otherwise, fur seal pup production and bowhead baleen seem to be recording events that originate with fluctuations in climate and propagate through the system.

Additional evidence of the sensitivity of fur seals to ecosystem state is found in patterns of growth in body size over time. In the past century, fur seals on St. Paul experienced periods of faster and slower growth (A. Trites unpubl. data), with each period lasting about as long as a climate regime (Figure 12). Faster growth occurred in regimes when common murres apparently predominated at Walrus I., a small island in the Pribilof

group where murres once nested in immense numbers: murres were eliminated by foxes that gained access to the island over winter ice in the early 1970s. Conversely, slow growth occurred in regimes when thick-billed murres apparently predominated. The well-documented alternation between murre species on Walrus I. (Peterson and Fisher 1955) also corresponded to shifts in climate regime (Springer 1998).

Fur seals are ecologically more similar to common murres than to thick-billed murres. That is, fur seals and common murres are more dependent on pelagic prey, whereas thick-billed murres incorporate a significant amount of benthic prey in their diets (Springer 1991; Sinclair et al. 1994; Springer et al. 1996). Therefore, the correspondence of positive responses of fur seals and common murres during periods when thick-billed murres apparently responded negatively is theoretically tractable.

Discussion

Functional relationships should always [why? Perhaps… typically have… is more realistic]have just one sign—positive or negative. Among the examples presented here, it is reasonable to believe that the common pattern of variability in meteorological conditions, as indexed by the NPI, and regional wind (observed atat St. Paul) represents a positive functional forcing-response relationship over the Bering Sea. It further can be argued that basin-scale meteorology and thus regional winds are influenced by changes in mean characteristics of the global scale ocean-atmosphere interactions. Variability in the Aleutian Low and elements of physical oceanography, such as transport through Bering Strait and the summer retreat of sea ice in the Chukchi Sea, must represent positive functional forcing-response relationships across the atmosphere-ocean interface.

In contrast to these single sign relationships, the sign of the relationship between wind and SST in the Bering Sea has alternated between generally negative and generally positive depending upon regime. A negative relationship might always be expected, since during much of the year wind mixes the upper layers of the ocean, countering effects of stratification and surface heating from the sun. Thus, it appears that while wind and SST in the Bering Sea may be adjacent ecosystem elements under certain conditions, under other conditions they may be separated by one or more other elements. Alternatively, it may be

that under certain conditions another element overrides the likely role of wind on SST, or perhaps wind and SST are responding independently to some other feature(s) of the physical system.

Similarly, it appears that the relationship between summer atmospheric forcing and summer retreat of sea ice was generally in phase during the 1950s through 1980s, but has been out of phase since. This may also represent the influence of another element dominating sea ice extent, e.g., an interaction with the Arctic Oscillation. Even during the long interval of positive correlation, the pattern of the NPI did not always exactly match that of summer sea ice extent, further implicating other factors in the full equation.

Physical variability would be expected to be reflected in biological variability. In the Bering Sea, the 50-y time series of $\partial^{13}C$ in bowhead whale baleen, an ostensible proxy of primary productivity, is well-correlated with the NPI and wind. At least two processes could explain these relationships, both of which begin with meteorology. One is that baleen $\partial^{13}C$ is mediated by wind, which plays major roles in primary and secondary production by creating turbulence that effects mixed layer and nutrient dynamics and feeding efficiencies of planktonic organisms and micronekton. Wind is clearly important to primary production in the Bering Sea (Sambrotto and Goering 1983; Sambrotto et al. 1986). Another possibility is the effect of atmospheric pressure on transport across the northern Bering-Chukchi shelf, where bowheads obtain the bulk of their annual nutrition (Sang 2001). Variability in northward transport leads to variability in primary production and the rate of advective supply of zooplankton (Springer et al. 1989; Springer and McRoy 1993) that might be reflected in the $\partial^{13}C$ of bowhead baleen.

Members of two contrasting food webs—deep basin pelagic (red-legged kittiwakes) and continental shelf pelagic (black-legged kittiwakes and juvenile pollock)—are extremely influenced by whatever it is that SST indexes. The most intriguing aspect of this is that the sign of the relationship between SST and juvenile pollock and kittiwakes changes between regimes, just as it does with SST and wind. These correlations probably should not be considered functional relationships in the strict sense, since there are potentially several ecological levels that are a bridge between them. It is more likely that SST serves as a proxy for one or more other features of the ecosystem that change in fundamental ways between regimes relative to SST that is/are responsible for the variability in abundance and

productivity of the birds and pollock. Still, in a predictive sense, SST is a powerful index provided one knows when a regime shifts.

SST was strongly predictive of age 3+ pollock biomass on the eastern shelf for over 2 decades and the sign was always positive regardless of regime, i.e., it did not change after 1989. The significance of the apparently negative relationship in the 1960s is unclear because of the uncertain effect of the rapidly developing commercial fishery on the relatively small virgin stock. However, the relationship may have again become negative since the mid-1990s. The reason for differences between trends in abundance of juvenile pollock and biomass of adult pollock in relation to trends in SST and regime are not readily apparent.

Just as signs of several relationships change over time as regimes shift, signs of trends in the abundance of seabirds and fur seals vary between habitats within regimes (Pribilofs/continental shelf *v* Bogoslof/oceanic) and ratios of congeneric murres on Walrus I. and growth rates of fur seals vary within habitat between regimes. In the case of fur seal growth rates, the effect is apparently manifested in the Gulf of Alaska as the seals return to the Bering Sea in spring (Trites and Bigg 1996). The geographic distance between locations where fur seal annual growth is determined and various parameters are measured in the Bering and Chukchi seas illustrates the spatial scale of influence of an overriding physical forcing factor, which is most likely the Aleutian Low pressure system.

In aggregate, there are numerous correlations among a variety of ecosystem components from fundamental meteorological forcing (the Aleutian Low pressure system) to primary physical response factors (winds, currents, and SST), to secondary physical and biological response parameters (sea ice extent, surrogate primary productivity, and the abundances and productivity of planktivorous fish and piscivorous marine birds and mammals). None of the physical-physical or physical-biological correlations proves cause and effect, but a considerable weight of evidence indicates that climate and climate change are extremely important in regulating production regimes in the Bering Sea. Routes through the ecosystem taken by these supposed chains of cause and effect are conjectural still, but several plausible scenarios come to mind. For example, fluctuating atmospheric pressure affects winds and currents that alter sea ice extent and primary productivity (as indexed by isotope ratios in bowhead baleen). Variable food web productivity, arising from the effect of

wind on primary productivity or on transfer efficiencies at low trophic levels, would be important at high trophic levels and could be expressed in fur seal growth, sea lion abundance, and alternating dominance of one or the other species of murre at Walrus I. The biological-biological correlations presented here demonstrate common responses to signals propagating through the ecosystem, rather than functional cause and effect relationships.

The emphasis of most recent analyses of effects of climate change has been on comparisons of mean parameter values or slopes, e.g., relatively higher or lower atmospheric pressure or increasing or decreasing abundance of a species, between regimes. That is, a given parameter in a given regime is reduced to a single value or sign (positive or negative). The data sets presented here show in addition a considerable amount of interannual coherence within and across regimes, supporting the notion that several may involve functional forcing-response relationships. Still, none of the supposed independent forcing variables, e.g., the summer atmospheric pressure field, explains all of the variability in the dependent response variables, e.g., summer sea ice retreat. In all cases, multiple forcing factors are at play.

Many things can affect any parameter value within a given year, such as measurement error and random events in the ecosystem. These can be important, for example as when a severe summer storm with high wind and heavy rain blows and washes away seabird chicks from nests, radically lowering productivity from a level that otherwise could have been supported by the system. Such random events are commonly unrelated to fundamental trends in forcing factors and can blur the picture of fundamental form. Thus, for example, the fundamental wave form of the longer term oscillation of summer NPI and sea ice, irrespective of regimes, can be more clearly seen when the data are smoothed as in Figure 1.

The relationships presented here implicate bottom-up control of various processes linking the Aleutian Low to seabirds and marine mammals. However, this should not be construed to mean that all demographic changes at high trophic levels represent responses to changing food web production and the availability of prey to responding species. In the case of fur seals, for example, variable growth rates likely do reflect changing prey abundance: declining pup production could be caused by declining carrying capacity affecting the ability of females to produce pups, or by the loss of females brought on by starvation (a prey

issue) or by predation. That species are sensitive to fluctuations in productivity of supporting food webs is not surprising, nor is it surprising that they are sensitive to changes in predation that might result from, or be exacerbated by, the same bottom-up pathways.

The tendency for the Bering Sea ecosystem to behave in particular ways depending upon seasonal, annual, and mean decadal physical forcing also is not surprising and is evident in numerous time series. What is less intuitive are explanations of the changing signs of relationships between elements of the ecosystem from one climate regime to another, such as between wind and SST and between SST and the productivity of pollock and kittiwakes. In all of these examples, other ecosystem elements must be involved in the actual functional relationships. Nevertheless, it is puzzling how the signs of these relationships change between positive and negative as climate regimes change. Whatever the explanation my prove to be, in the meantime it is important to be mindful of the potential for inconstant polarity, relative not only to time but to other ecosystem attributes. It is especially important when attempting to develop ways to predict an outcome, such as pollock production, based on one or a combination of indices. Ecosystems apparently do have memory, or inertia, but the path taken by ecosystem processes is steered in different directions under different climate situations, thus changing outcomes in ways that are surprising and unpredictable.

References

Anderson, P.J. and J.F. Piatt. 1999. Community reorganization in the Gulf of Alaska following ocean climate regime shift. Mar. Ecol. Progr. Ser. 189: 117-123.

Beamish, R.J.e. 1995. Climate change and northern fish populations. Can. Spec. Pub. Fish. Aquat. Sci. 121: 739.

Coachman, L.K., K. Aagaard, and R.B. Tripp. 1975. Bering Strait: regional physical oceanography. Seattle, WA, University of Washington Press. 172 pp.

Dragoo, D.E., G.V. Byrd, and D.B. Irons. 2001. Breeding status, population trends and diets of seabirds in Alaska, 2000. U.S. Fish and Wildl. Serv. Rep. AMNWR 01/07, 77 pp.

Ebbesmeyer, C.C., D.R. Cayan, F.H. McLain, D.H. Peterson, and K.T. Redmond 1991. 1976 step in the Pacific climate: forty environmental changes between 1968-1975 and 1977-1985. In Proceedings of the Seventh Annual Pacific Climate Workshop. Interagency Ecological Studies Program Tech. Rep. 26. J.L. Betancourt and V.L. Tharp. Sacramento, CA, California Department of Water Resources, p. 129-141.

Francis, R.C., S.R. Hare, A.B. Hollowed, and W.S. Wooster. 1998. Effects of interdecadal climate variability on the oceanic ecosystems of the NE Pacific. Fish. Oceanogr. 7: 1-21.

Hare, S.R., N.J. Mantua, and R.C. Francis. 1999. Inverse production regimes: Alaskan and West Coast Pacific salmon. Fisheries 24: 6-14.

Klyashtorin, L.B. and F.N. Rukhlov. 1998. Long-term climate change and pink salmon stock fluctuations. N. Pac. Anadr. Fish Comm. Bul 1: 464-479.

Mackas, D.L., R. Goldblatt, and A.G. Lewis. 1998. Interdecadal variation in developmental timing fo *Neocalanus plumchrus* populations at Ocean Station P in the subarctic North Pacific. Can. J. Fish. Aquat. Sci. 55: 1878-1893.

Mantua, N.J., S.R. Hare, Y. Zhang, J.M. Wallace, and R.C. Francis. 1997. A Pacific interdecadal climate oscillation with impacts on salmon production. Bull. Amer. Meteoro. Soc. 78: 1069-1079.

Minobe, S, 1999. Resonance in bidecadal and pentadecadal climate oscillations over the North Pacific: Role in climate regime shifts. Geophys. Res. Lets., 26(7), 853-858.

McGowan, J.A. 1990. Climate and change in oceanic ecosystems: the value of time-series data. Trends Ecol. Evol. 5: 293-299.

Niebauer, H.J. 1998. Variability in Bering Sea ice cover as affected by a regime shift in the north Pacific in the period 1947-96. J. Geophys. Res. 103: 27717-27737.

NMML. 1994. Status review of Steller sea lions (*Eumetopias jubatus*), National Marine Mammal Laboratory, National Marine Fisheries Service, NOAA, Seattle, Washington. 40 pp.

Peterson, R.T. and J. Fisher. 1955. Wild America. Boston, Houghton Mifflin Co. 434 Polovina, J.J., G.T. Mitchum, and G.T. Evans. 1995. Decadal and basin-scale variations in mixed layer depth and the impact on biological production in the Central and North Pacific. Deep-Sea Research 42: 1701-1716.

Sambrotto, R.N. and J.J. Goering 1983. Interannual variability of phytoplankton and zooplankton production on the southeast Bering Sea shelf. In From year to year. W.S. Wooster. Seattle, Washington, Washington Sea Grant, p. 161-177.

Sambrotto, R.N., H.J. Niebauer, J.J. Goering, and R.L. Iverson. 1986. Relationships among vertical mixing, nitrate uptake, and phytoplankton growth during the spring bloom in the southeast Bering Sea middle shelf. Cont. Shelf Res. 5: 161-198.

Schell, D.M. 2000. Declining carrying capacity in the Bering Sea: Isotopic evidence from whale baleen. Limnol. Oceanogr. 45: 459-462.

Schumacher, J.D., N. A. Bond, R. D. Brodeur, P. A. Livingston, J. M. Napp and P. J. Stabeno, in press. Climate Change in the Southeastern Bering Sea and Some Consequences for Biota. In: Large Marine Ecosystems of the World: Trends in Exploitation, Protection, and Research. G. Hempel, K. Sherman, editors. Amsterdam: Elsevier Science.

Sinclair, E., T. Loughlin, and W. Pearcy. 1994. Prey selection by northern fur seals (*Callorhinus ursinus*) in the eastern Bering Sea. Fish. Bull. 92: 144-156.

Springer, A.M. 1991. Seabird relationships to food webs and the environment: examples from the North Pacific Ocean. In Studies of high-latitude seabirds. 1. Behavioral, energetic, and oceanographic aspects of seabird feeding ecology. W.A. Montevecchi and A.J. Gaston. Ottawa, Canadian Wildlife Service, p. 39-48.

Springer, A.M. 1998. Is it all climate change? Why marine bird and mammal populations fluctuate in the North Pacific. In Biotic impacts of extratropical climate variability in the Pacific. Proceedings 'Aha Huliko'a Hawaiian Winter Workshop. G. Holloway, P. Muller and D. Henderson. Honolulu, HI, University of Hawaii, p. 109-119.

Springer, A.M. and C.P. McRoy. 1993. The paradox of pelagic food webs in the northern Bering Sea-III. Patterns of primary production. Cont. Shelf Res. 13: 575-599.

Springer, A.M., C.P. McRoy, and K.R. Turco. 1989. The paradox of pelagic food webs in the northern Bering Sea—II. Zooplankton communities. Cont. Shelf Res. 9: 359-386.

Springer, A.M., J.F. Piatt, and G.B. Van Vliet. 1996. Seabirds as proxies of marine habitats and food webs in the western Aleutian Arc. Fish. Oceanogr. 5: 45-55.

Stabeno, P.J. and J.E. Overland, 2001. Bering Sea shifts toward an earlier spring transition. *EOS*, Transactions of the American Geophysical Union, Vol. 29, pg. 317, 321.

Stabeno, P.J., N. A. Bond, N. B. Kachel, S. A. Salo, and J. D. Schumacher, 2001. Temporal Variability in the Physical Environment over the Southeastern Bering Sea. *Fish. Oceanogr., 10*: 81-98.

Trenberth, K.E. and J.W. Hurrell. 1994. Decadal atmospheric-ocean variations in the North Pacific. Clim. Dynam. 9: 303-319.

Trites, A.W. and M.A. Bigg. 1996. Physical growth of northern fur seals: seasonal fluctuations and migratory influences. J. Zool. (Lond.) 238: 459-482.

Trites, A.W. and P.A. Larkin. 1996. Changes in the abundance of Steller sea lions (Eumetopias jubatus) in Alaska from 1956 to 1992: how many were there? Aquat. Mamm. 22: 153-166.

Welch, D.W., B.R. Ward, B.D. Smith, and J.P. Eveson 1998. Influence of the 1990 ocean climate shift on British Columbia steelhead (O. mykiss) and coho (O. kisutch) populations. In Biotic impacts of extratropical climate variability in the Pacific. Proceedings 'Aha Huliko'a Hawaiian Winter Workshop. G. Holloway, P. Muller and D. Henderson. Honolulu, HI, University of Hawaii, p. 77-87.

Wyllie-Echeverria, T. and W.S. Wooster. 1998. Year-to-year variations in Bering Sea ice cover and some consequences for fish distributions. Fish. Oceanogr. 7: 159-170.

York, A.E. and J.R. Hartley. 1981. Pup production following harvest of female northern fur seals. Can. J. Fish. Aquat. Sci. 38: 84-90.

York, A.E. and P. Kozloff. 1987. On the estimation of numbers of northern fur seal, *Callorhinus ursinus*, pups born on St. Paul Island, 1980-86. Fish. Bull. 85: 367-375.
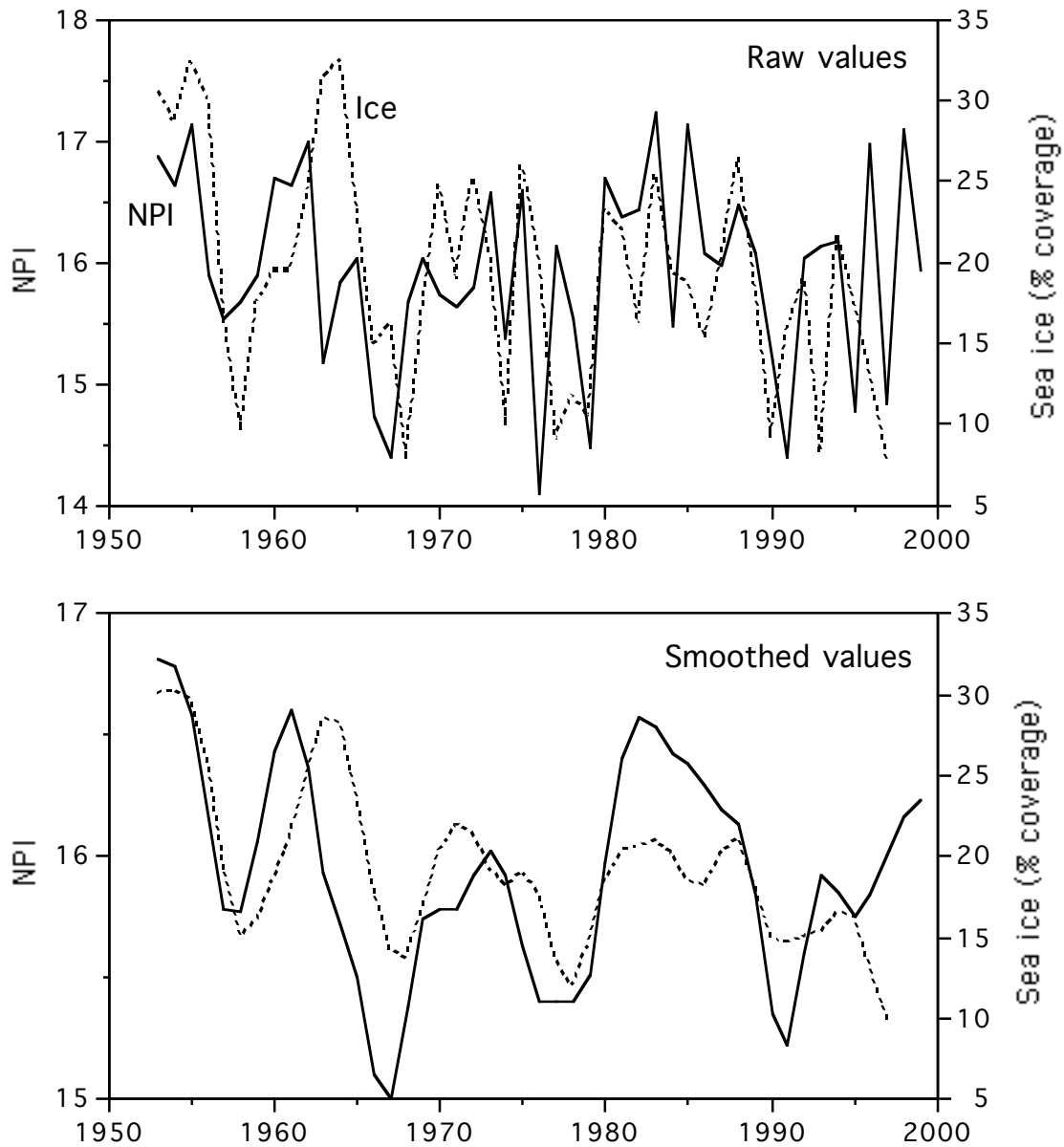
FIGURES AND TABLES

Figure 1. Summer extent of sea ice scaled as percent coverage of the Chukchi-Bering shelf (see Niebauer 1998) and mean July-September NPI.
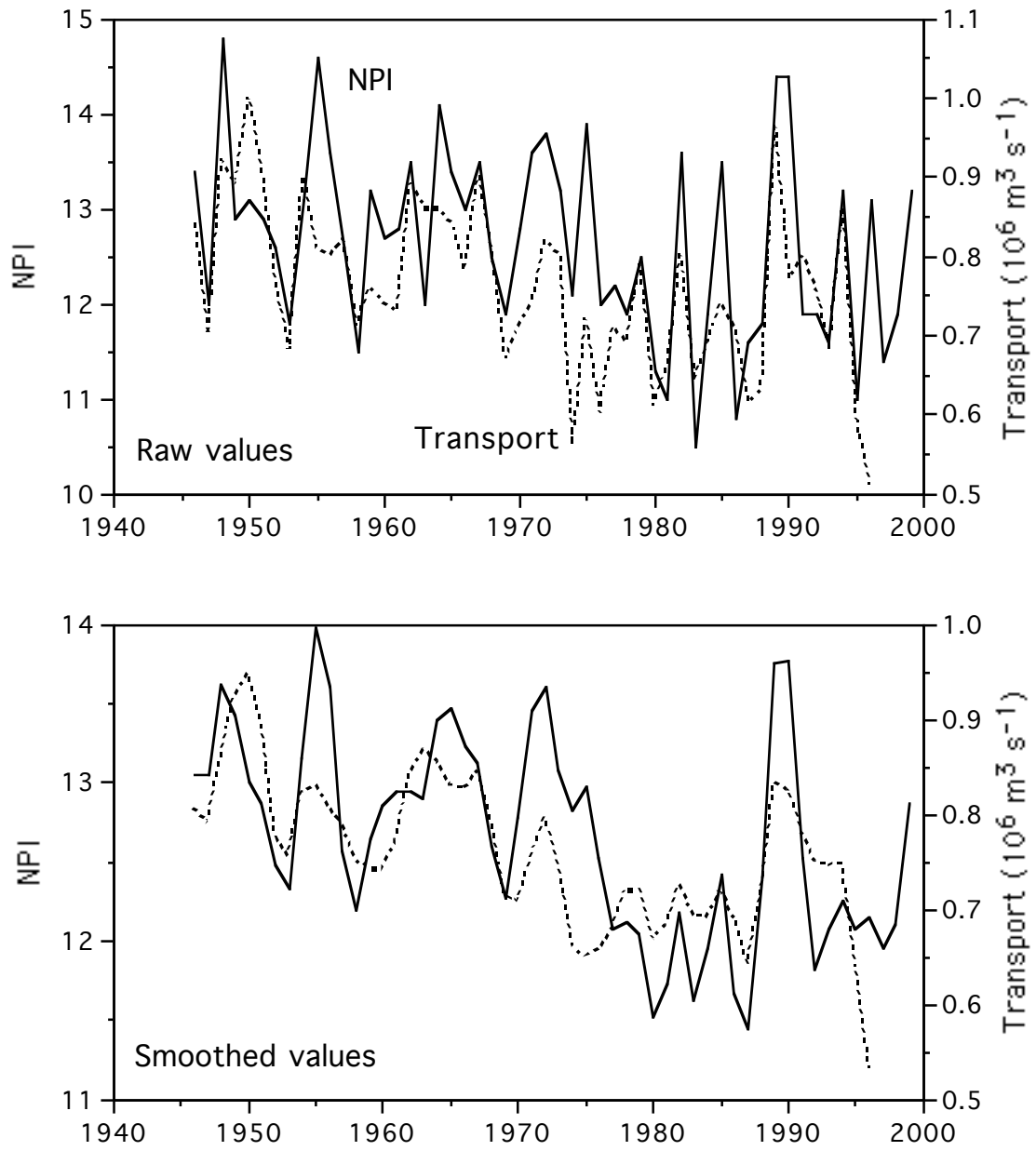
Figure 2. Annual northward transport through Bering Strait and the mean annual NPI.
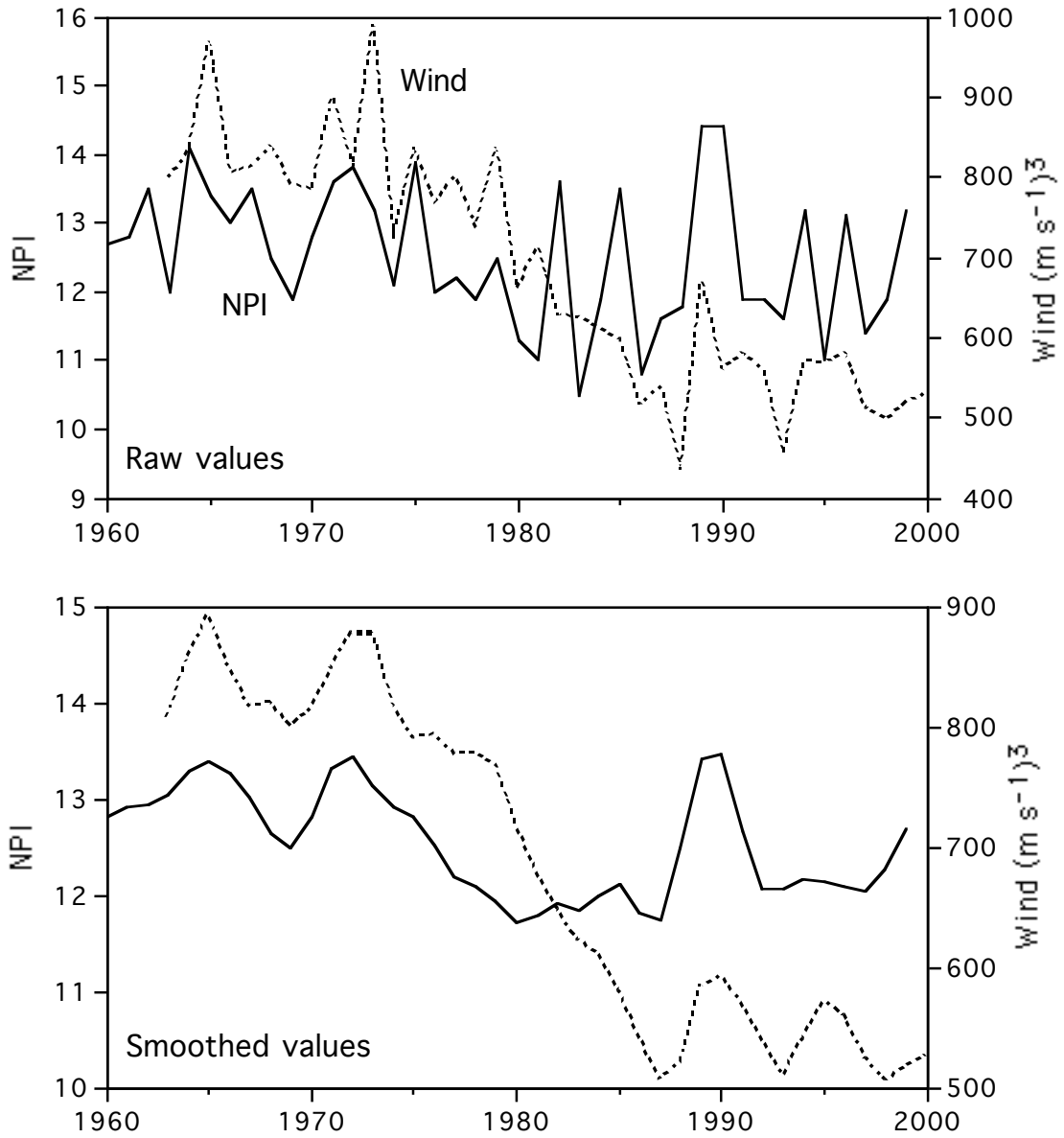
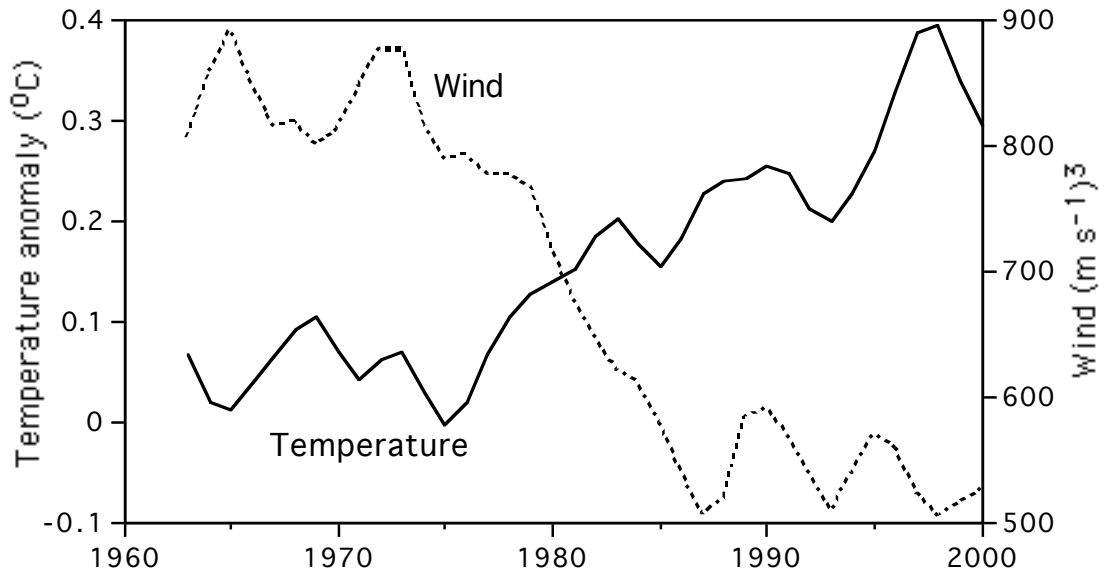Figure 3. Mean annual wind at St. Paul and the NPI.

Figure 4. Mean annual wind at St. Paul and the global ocean temperature anomaly. Wind data smoothed.
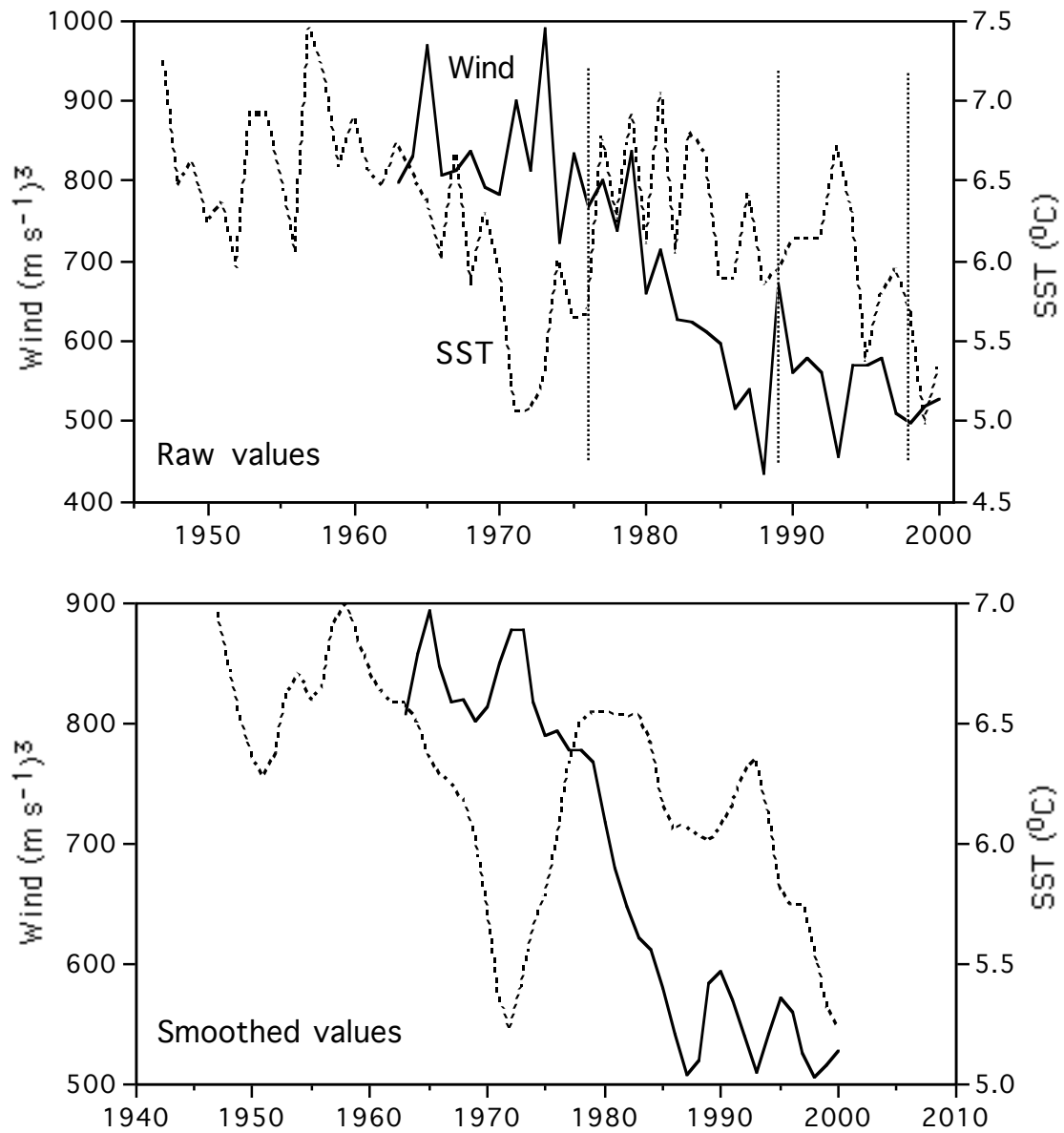
Figure 5. Mean annual wind at St. Paul and sea surface temperature (SST) in the eastern Bering Sea. Vertical lines show regime shifts in 1977, 1989, and 1998.
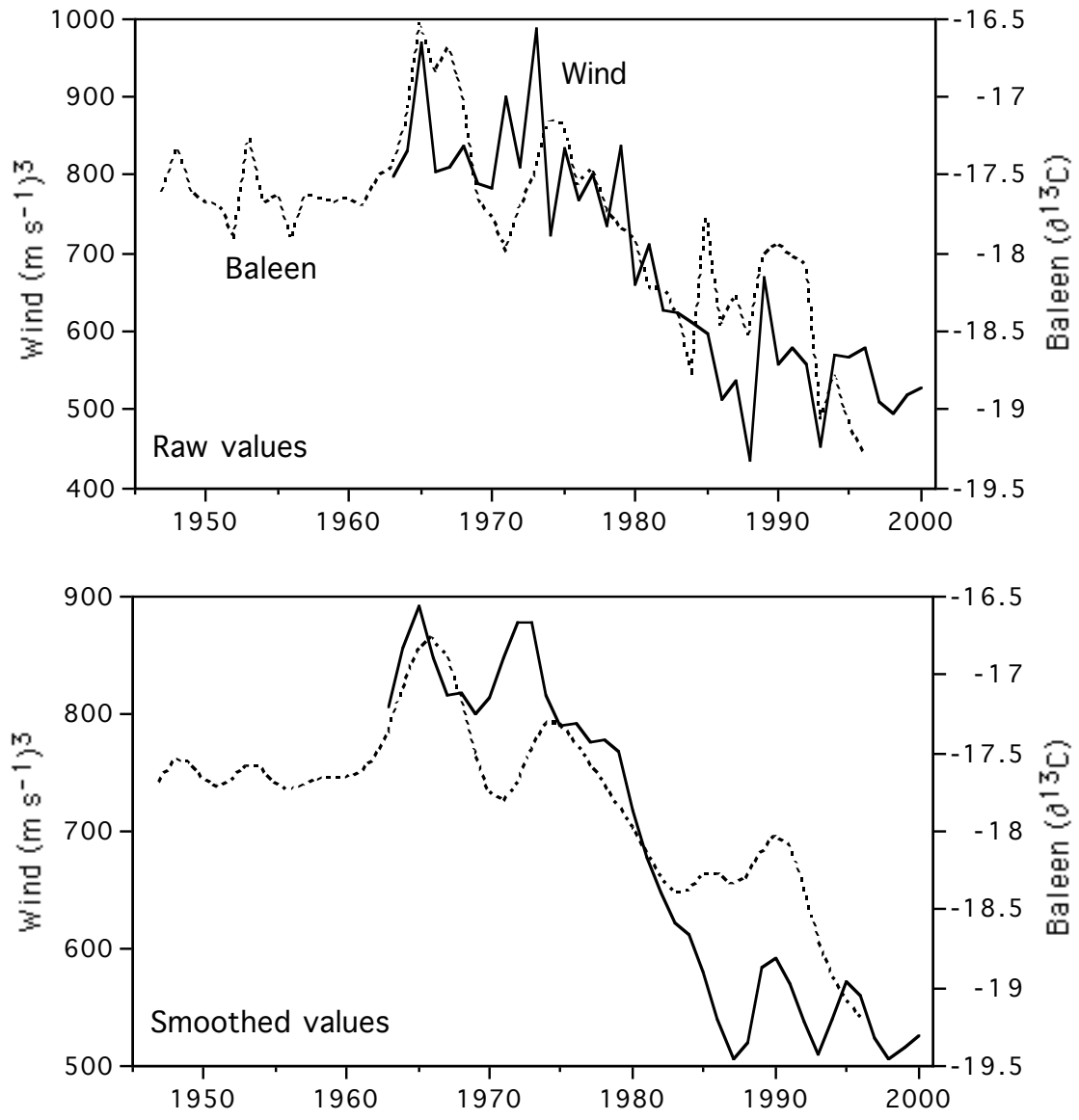
Figure 6. Bowhead whale baleen $\partial^{13}C$ (lagged 1 year) and mean annual wind at St. Paul.
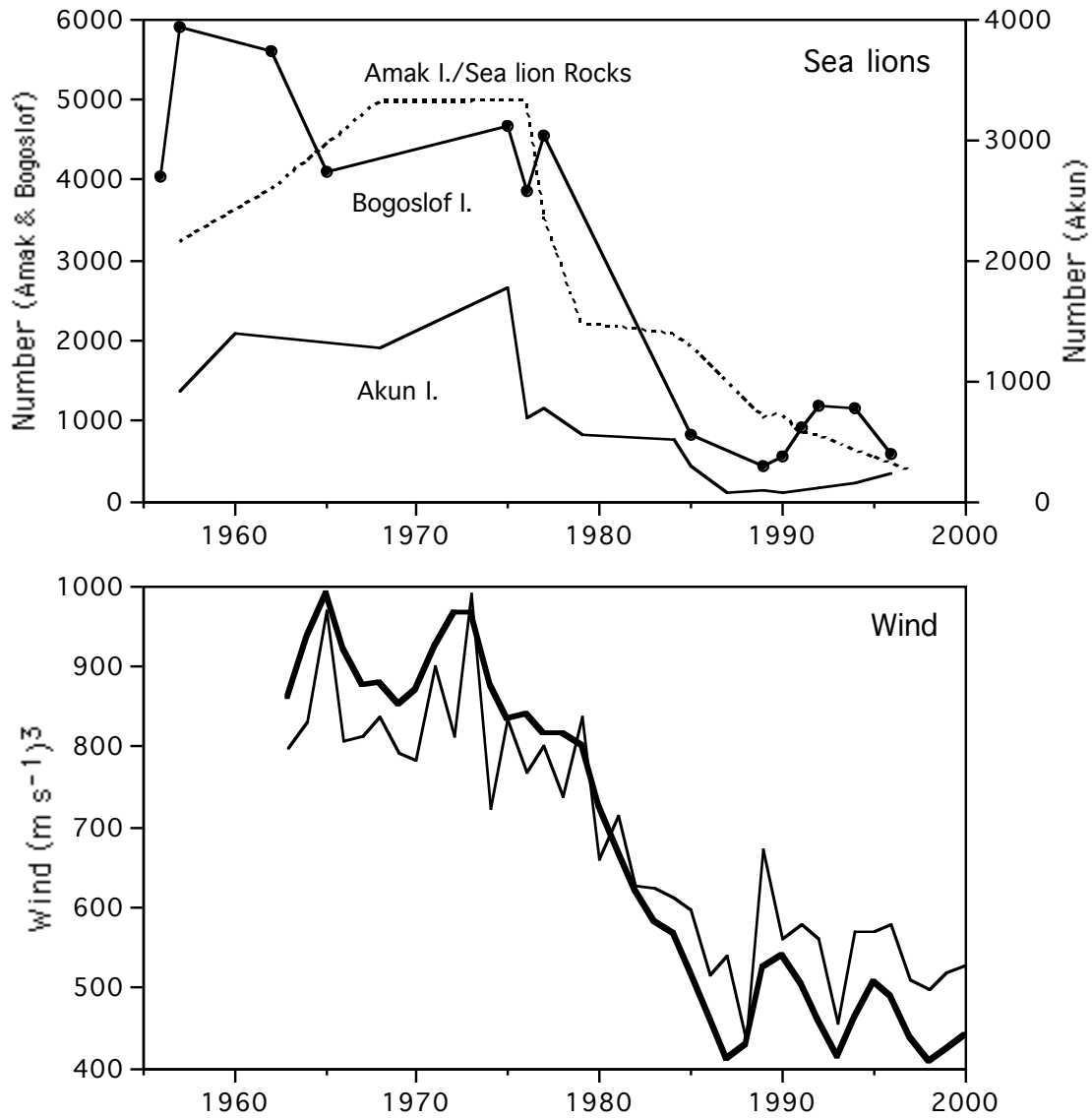
Figure 7. Sea lion abundance at rookeries in the eastern Aleutian Is. and wind at St. Paul I. Heavy line in wind panel is the smoothed trend.
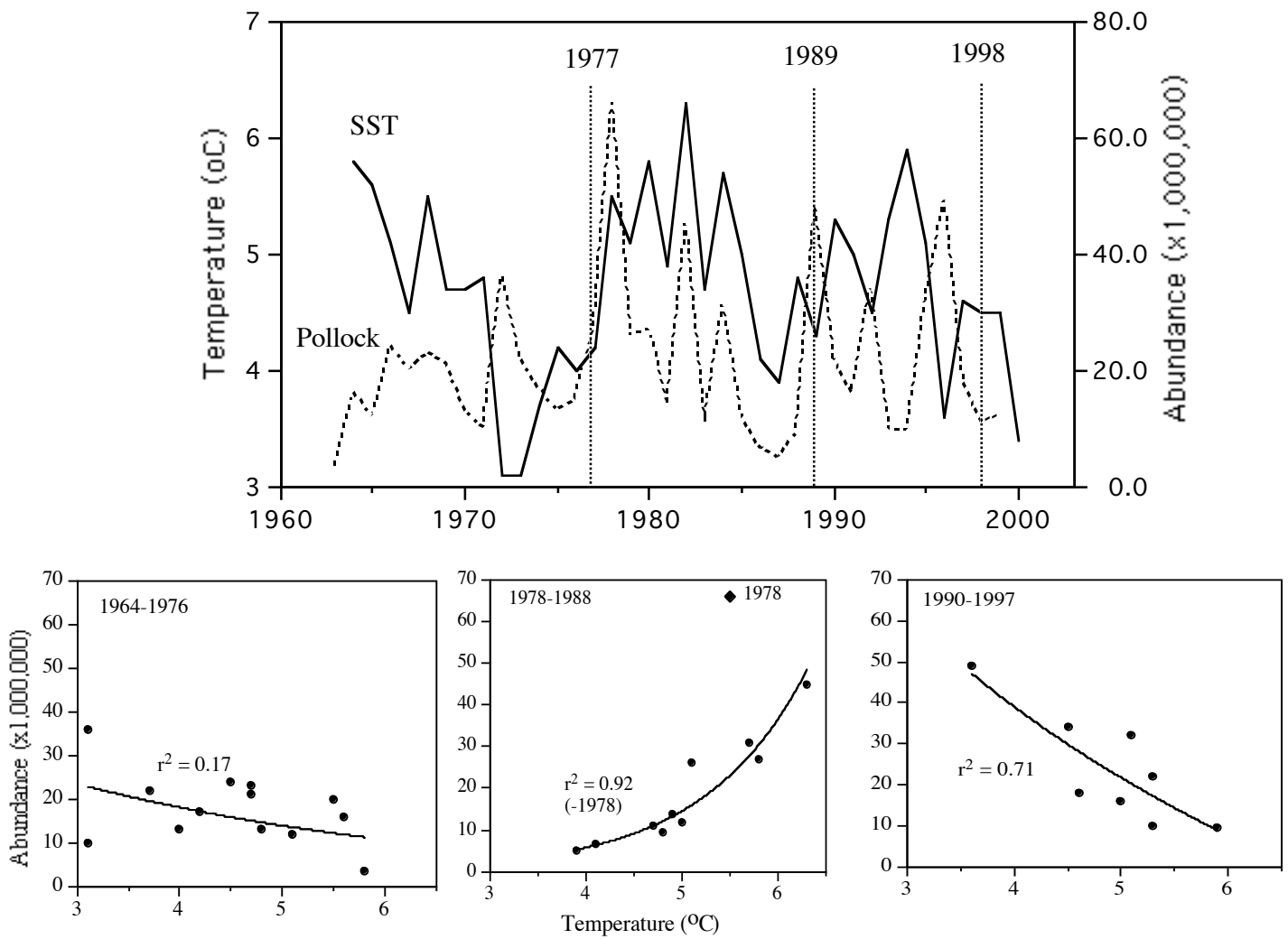
Figure 8. Abundance of age 1+ pollock and mean April-June sea surface temperature (SST: lagged 1 year) on the eastern Bering Sea shelf. The transition years (1977,1989 and 1998) are not included in the regression and as is 1978 since it was an extreme in recruitment.
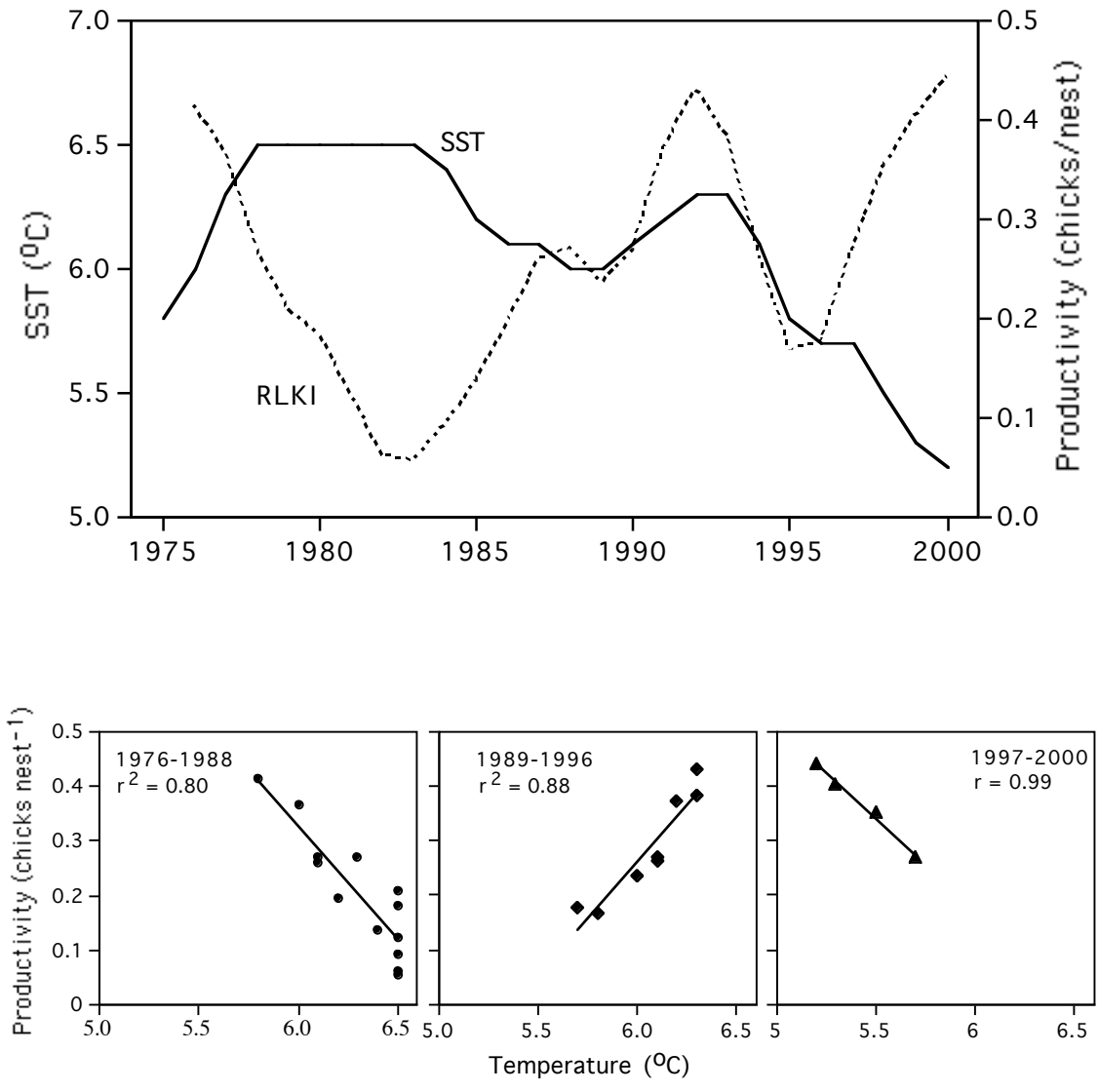
Figure 9. Red-legged kittiwake productivity at St. George I. and mean annual sea surface temperature (SST) in the eastern Bering Sea. Smoothed trends. A similar relationship exists for black-legged kittiwakes.
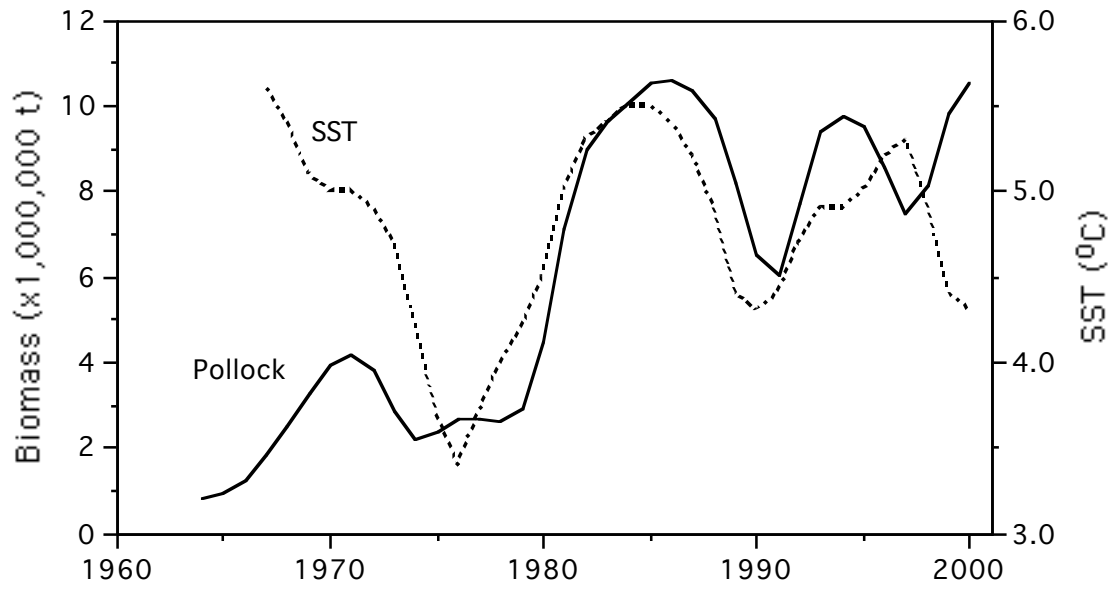
Figure 10. Biomass of age 3+ pollock in the eastern Bering Sea and mean April-June sea surface temperature (SST: lagged 4 years). Smoothed trends.
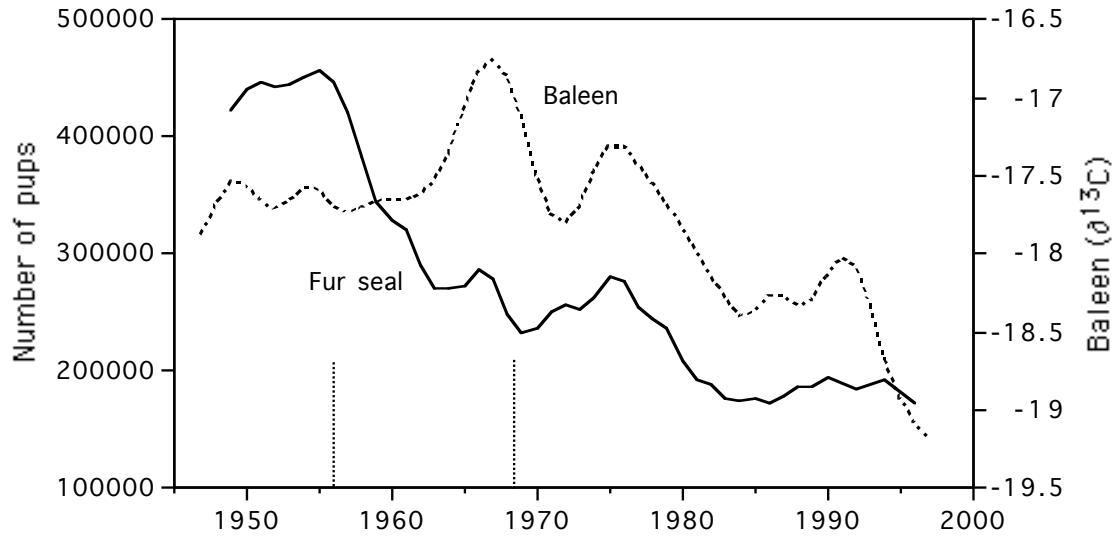
Figure 11. Fur seal pup production on St. Paul I. and isotope ratios in bowhead whale baleen. Smoothed trends. Dotted vertical lines at 1956 and 1968 mark interval of experimental female harvest.

Figure 12. Fur seal growth at St. Paul I. and the relative abundance of common and thick-billed murres on Walrus I. Dotted vertical lines show mark regime shifts in 1925, 1947, and 1977 (Mantua and Hare 1997). Adapted from Springer (1998). Heavy line is smoothed trend.

Table 1. Trends in populations of seabirds and fur seals at four locations in the Bering Sea.

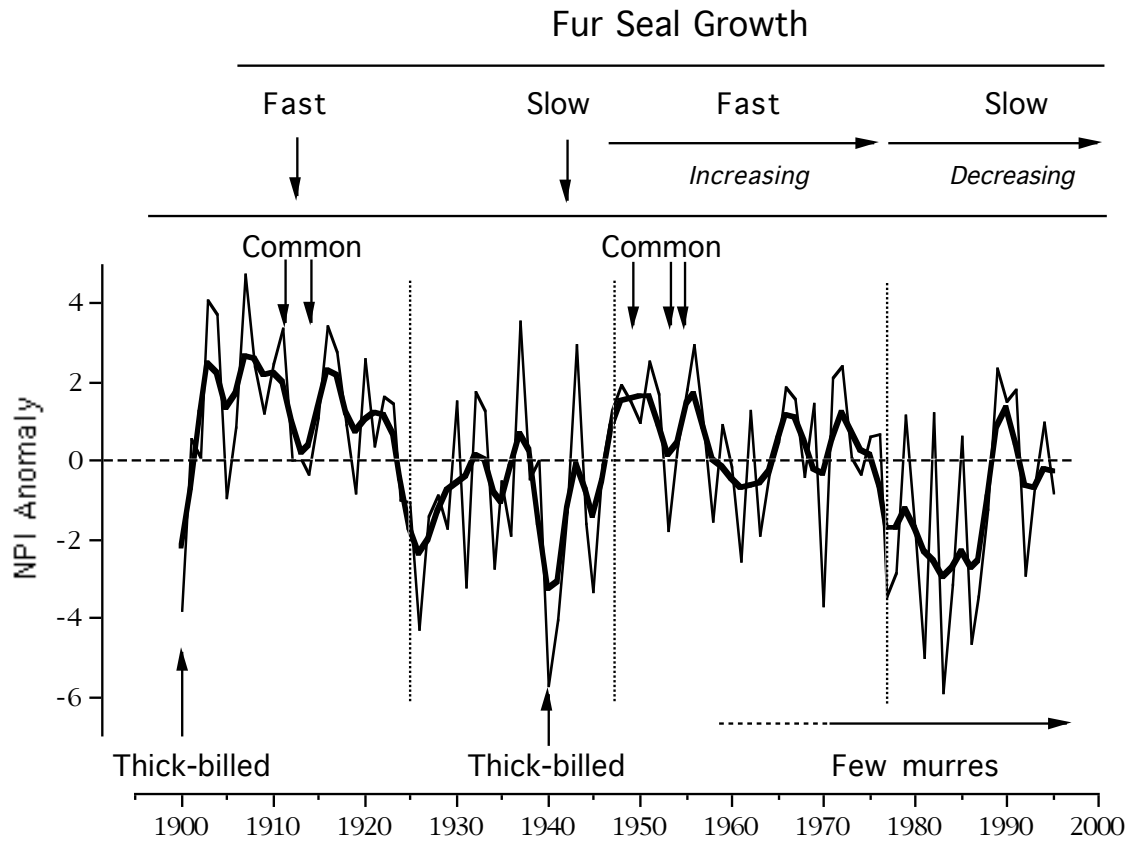| Location	Species	Interval	n	% Change	r^2
St. Paul I.					
(Pribilofs)	Black-legged Kittiwake	1976-1999	12	-73	0.79
	Red-legged Kittiwake	1976-1999	12	-70	0.72
	Common Murre	1976-1999	12	-62	0.62
	Thick-billed Murre	1976-1999	12	-44	0.72
	Northern Fur Seal	1975-2000	24	-37	0.6
	Mean (SE)			**-57 (7.1)**	
St. George I.					
(Pribilofs)	Black-legged Kittiwake	1976-1999	11	-47	0.45
	Red-legged Kittiwake	1976-1999	11	-52	0.63
	Common Murre	1976-1999	11	+55	0.56
	Thick-billed Murre	1976-1999	11	0	-
	Northern Fur Seal	1975-2000	24	-70	0.84
	Mean (SE)			**-23 (23)**	
Bogoslof I.					
(E Aleutians)	Black-legged Kittiwake	1973-2000	3	+150	0.8
	Red-legged Kittiwake	1973-2000	3	+550	0.95
	Tufted Puffin	1973-2000	5	+130	0.98

64

	Northern Fur Seal	1980-1997	12	+2500	0.98
	Mean (SE)			**+832 (564)**	
Buldir I.					
(W	Black-legged	1974-1996	10	+450	0.84
Aleutians)	Kittiwake				
	Red-legged	1974-1996	10	+200	0.81
	Kittiwake				
	Thick-billed Murre	1974-1996	10	+320	0.91
	Mean (SE)			**+323 (72)**	

6. FURTHER DEVELOPMENT OF INDICES IN THE EASTERN BERING SEA

Based on the results from 4 workshops, the members of the IWG believe that the following are logical next steps in the development and refinement of indices. These suggestions have been grouped into two categories: indices that are related to changes in strength of a given year-class of pollock and an index that may provide guidance regarding interpretation of the annual stock assessment from trawl results. While this later category was not in the original the charge to the IWG or a focus of SEBSCC, it is an vital component of fishery management.

Indices for estimating recruitment of age-1 pollock:

Continue comparisons with other model simulations and observations to provide verification of the Bering Sea Model (NEPROMS).

Develop a wind index of nutrient supply to the shelf from Bering Canyon.

Develop interface and/or other techniques so the NEPROMS can is more accessible as a tool.

Examine various indices versus occurrence of northwest and southeast centers of the adult pollock population.

Extract an index of zooplankton abundance from ECOSYM

Develop history of the time/space occurrence of the roe fishery to help define time/space limits for pollock eggs as initial points for trajectory simulations.

Develop a similar product for spawning that occurs in the vicinity of Bogoslof Island.

Use temperature observations from annual trawl survey to develop an index of the presence of the cold pool and the locations of the inner and middle fronts (i.e., the boundaries of the middle shelf domain in a given year.

Use temperature observations to create annual distributions of temperature, which in turn can be used to simulate zooplankton production.

An Index for interpretation of the annual stock assessment:
Examine influence of changes in the physical environment (e.g., water temperature, location of fronts) on preferred habitat for pollock and how variations in these features might affect estimates from trawl results.

Simulations from the NEPROMS are vital to further development of indices for the Bering Sea ecosystem. Continued verification of simulations (both velocity and water property fields) from this model and improvements to its physics (i.e., including northward flow through Bering Strait) has the highest priority. The development of a wind related index of potential nutrient transport shoreward along the Alaskan Peninsula from Bering Canyon and can be accomplished independent of the NEPROMS. Comparisons between OSCURS and NEPROMS (Section 3.?) demonstrate that dynamics other than direct wind forcing are critical throughout most of the water column. Thus, model simulations of the

integrated flux through appropriate cross sections, would provide a more complete measure of nutrient flux. Model simulations can also be used to establish temperature distributions at a time perhaps more appropriate (May-June) than the data from the trawl survey (July-August) for making estimates of zooplankton production.

Given the overall important of using NEPROMS simulations to help us understand physical mechanisms and their impact on biota, the utility of this model must be improved. In addition, as techniques/understanding of dynamics improves, this model should be updated to include as much physics as is possible. How can the NEPROMS become a user-friendlier tool? This may take the form of having made and stored average (likely daily) water property and velocity field distributions. If these simulations were then coupled with an interactive interface, which would allow a naive user to choose particular simulations and then access them in selected time/space domains, then the NEPROMS would permit far more research into indices and questions of how the ecosystem functions then is possible today.

7. REFERENCES

Brodeur, R.D., P.A. Livingston, T.R. Loughlin and A.B. Hollowed (eds.), 1996. Ecology of juvenile walleye pollock, *Theragra chalcogramma*. NOAA Technical Report NMFS 126, 227 pp.

Francis, R.C., S.R. Hare, A.B. Hollowed, and W.S. Wooster, 1998. Effects of interdecadal climate variability on the oceanic ecosystems of the NE Pacific. *Fish. Oceanogr.*, *7*, 1–21.

Francis, R.C. and K.M. Bailey, 1983. Factors affecting recruitment of selected gadiods in the northeastern Pacific and east Bering Sea. *In:* Year to Year Interannual Variability of the Environment and Fisheries of the Gulf of Alaska and the Eastern Bering Sea. Pp. 17-22, Ed. By W. S. Wooster, Washington Sea Grant, University of Washington, Seattle, WA, USA.

Ianelli, J., L.W. Fritz, T. Honkalehto, N. Williamson and G. Walters. 1998. Eastern Bering Sea walleye pollock stock assessment with yield considerations for 1999. *In:* Stock Assessment and Fishery Evaluation Report for the Groundfish Resources of the Bering Sea/Aleutian Islands Regions, pp. 31-111. Ed by Groundfish Plan Team for the Bering Sea-Aleutian Islands Region, North Pacific Fishery Management Council, 605 W 4th Ave., Suite 306, Anchorage, AK. 99501. 560 pp.

Ingraham, W.J. Jr. and R.K. Miyahara, 1988. Ocean surface current simulations in the North Pacific Ocean and Bering Sea (OSCURS-Numerical Model). US Department of Commerce, National Oceanic and Atmospheric Administration, Technical Memorandum, National Marine Fisheries Service F/NWC-130. 155 pp.

Kachel, N. B., S. A. Salo, J. D. Schumacher, P. J. Stabeno and T. E. Whitledge, in press. Characteristics of the Inner Front of the Southeastern Bering Sea. *Deep Sea Res., Topical Studies in Oceanogr*

Livingston, P.A., 1993. The importance of predation by groundfish, marine mammals, and birds on walleye pollock *Theragra chalcogramma* and Pacific herring *Clupea pallasi* in the eastern Bering Sea. *Mar. Ecol. Prog. Ser. 102*, 205–215.

Livingston, P.A., and R.D. Methot, 1998. Incorporation of predation into a population assessment model of eastern Bering Sea walleye pollock. *In*: Fishery Stock Assessment Models, Alaska Sea Grant College Program, AK-SG-98-01: 16 pp.

Megrey, B.H., A.B. Hollowed, S.R. Hare, S.R. Macklin andP.J. Stabeno, 1996. Contribution of FOCI researchto forecasts of year-class strength of walleye pollock in Shelikof Strait, Alaska. *Fisheries Oceanogr., 5 (Suppl.1)*, 189-203.

Napp, J.M., A.W. Kendall, Jr., and J.D. Schumacher, 2000. A synthesis of biological and physical processes affecting the feeding environment of larval walleye pollock (*Theragra chalcogramma)* in the eastern Bering Sea. *Fish. Oceanogr. 9*:147-162

NRC (National Research Council), 1996. The Bering Sea Ecosystem. National Academy Press, Washington, D.C., 324 pp.

Reed, R.K., 1999. A time series of temperature, salinity, and geopotential across the southeastern Bering Sea shelf, 1995–1999. NOAA Tech. Report ERL 455-PMEL 43 (NTIS PB2000-100564), 15 pp.

Rosenkranz, G.E., A.V. Tyler and G.H. Kruse, 2001. Effects of water temperature and wind on year - class strength of Tanner crabs in Bristol Bay, Alaska. *Fish. Oceanogr. 10, 1:* 1-12.

Schumacher, J.D., N. A. Bond, R. D. Brodeur, P. A. Livingston, J. M. Napp and P. J. Stabeno, in press. Climate Change in the Southeastern Bering Sea and Some Consequences for Biota. In: *Large Marine Ecosystems of the World: Trends in Exploitation, Protection, and Research*. G. Hempel, K. Sherman, editors. Amsterdam: Elsevier Science.

SEBSCC Concept Paper, 1995

Schumacher, J.D., and P. J. Stabeno, 1998. Continental shelf of the Bering Sea. *In*: The Sea: Vol. 11-The Global Coastal Ocean: Regional Studies and Synthesis, John Wiley &Sons, Inc, New York, NY, 789-822.

Schumacher, J.D., and P.J. Stabeno, 1994. Ubiquitous eddies of the eastern Bering Sea and their coincidence with concentrations of larval pollock. *Fish. Oceanogr. 3*, 182–190.

Springer, A.M., and G.V. Byrd, 1989. Seabird dependence on walleye pollock in the southeastern Bering Sea. *In:* Proceedings of the International Symposium on the Biology and Management of Walleye Pollock. Alaska Sea Grant, AK-SG-89-01, pp. 667–677.

Stabeno, P.J., N. A. Bond, N. B. Kachel, S. A. Salo, and J. D. Schumacher, 2001. Temporal Variability in the Physical Environment over the Southeastern Bering Sea. *Fish. Oceanogr*. *10*: 81-98.

Stabeno, P.J., N.B. Kachel, M. Sullivan, and T.E. Whitledge, 2002. Variability along the 70-m isobath of the southeast Bering Sea. *Deep Sea Res., II: Topical Studies in Oceanography,* **49**, 5931–5943.

Stabeno, P.J., J.D. Schumacher, and K. Ohtani, 1999. Physical oceanography of the Bering Sea. *In*: Loughlin, T. R., and K. Ohtani (eds.), Dynamics of The Bering Sea: Physical, Alaska Sea Grant College Program, Fairbanks, AK. 1-28.

Tyler, A.V and A.B. Hollowed, 2001. Groundfish trends in the eastern Bering Sea. Prepared for the SEBSCC Synthesis Group, pp. 11.

Wespestad, V.G., L.W. Fritz, W.J. Ingraham, Jr., and B.A. Megrey, 2000. On relationships between cannibalism, climate variability, physical transport and recruitment success of Bering Sea walleye pollock, *Theragra chalcogramma. ICES J. Mar. Sci. 57:* 272-278.